

**DRY POWDER INHALERS FOR THE TREATMENT OF ASTHMA:
AN ENGINEERS APPROACH**

Bradley Yip

Bachelor of Engineering
With a Major In Mechanical Engineering



Department of Mechanical Engineering
Macquarie University

November 7, 2016

Supervisor: Dr. Agisilaos Kourmatizis
Co-Supervisor: Dr. Shaokoon Cheng



ACKNOWLEDGMENTS

I would like to acknowledge my supervisor Agisilaos Kourmatzis for his help and guidance, DFE Pharma for providing the powders for testing and Macquarie University for the opportunity and resources.



STATEMENT OF CANDIDATE

I, Bradley Yip, declare that this report, submitted as part of the requirement for the award of Bachelor of Engineering in the Department of Mechanical Engineering, Macquarie University, is entirely my own work unless otherwise referenced or acknowledged. This document has not been submitted for qualification or assessment at any academic institution.

Student's Name: Bradley Yip

Student's Signature:

Date: 7/11/2016



ABSTRACT

Dry Powders inhalers (DPIs) are an increasingly popular method of treatment for the symptoms of Asthma and Chronic Pulmonary Disease (COPD). However due to the nature of DPIs complicated drug delivery system, research into the development and improvement provides a significant challenge. While there are many different devices available on the market, none of these provide consistent delivery for varying inhalation profiles. This variability is determined by the drug formulation, the design of the device and the patient's inhalation profile. This paper focuses on the proof of concept and early results of research into a systematic study of the influence of the physicochemical properties of the carrier particles, and the nature of the fluid flow, on powder fragmentation and transport. This thesis paper will be particularly useful for the researchers furthering this study and the industry partner DFE Pharma. The research was conducted through a controlled flow that was fed into a unique rig, with measurements taken from a laser photodiode setup. The results found that the majority of data that be achieved is located around the far end of the pocket in respective to the flow and follows known correlations between size and evacuation times.



Contents

Acknowledgments	iii
Abstract	vii
Table of Contents	ix
List of Figures	xiii
List of Tables	xv
1 Introduction	1
1.1 Objectives	2
1.2 Limitations	2
1.2.1 Time	2
1.2.2 Cost	3
1.2.3 Materials	3
1.3 Project plan	3
1.4 Risk Assessment	4
2 Background and Related Work	5
2.1 Introduction	5
2.1.1 Importance	5
2.1.2 Chronic Airway Disease	6
2.2 Dry Powder Inhalers	8
2.2.1 Entrainment	9
2.2.2 Carriers	9
2.2.3 Particle Size	9
2.3 Current Research Techniques	10
2.4 Current Research	10
2.4.1 Design of Device	12
2.4.2 Physicochemical Properties and Morphology	13
2.4.3 Effect of Air Flow	15
2.4.4 Patient Training	15
2.4.5 New Novel Devices	15

2.5	Conclusion	16
3	Approach and Testing	17
3.1	Introduction	17
3.1.1	Theoretical Calculations	18
3.2	Parts	20
3.2.1	Materials	23
3.2.2	Reason for Selection	23
3.3	Assembling of Equipment	23
3.3.1	Remodeled Sections	23
3.3.2	Acquiring and Controlling the Air Flow	25
3.3.3	DPI Rig	26
3.3.4	Testing Components	29
3.3.5	Software Programs and Data Analysis	30
3.4	Testing	32
3.4.1	Hot Wire Testing	32
3.4.2	Laser Setup and Measurements	33
4	Results	35
4.1	hotwire	35
4.2	Laser Tests	38
4.2.1	Control	38
4.2.2	Sample Rates and Time Flowing	40
4.2.3	Locating Detectable Data	41
4.2.4	Laser Directed Through The Pocket	44
5	Discussion	47
5.1	Rig Analysis	47
5.1.1	Remodeled Sections	47
5.1.2	Acquiring and Controlling the Air Flow	48
5.1.3	Testing Components	48
5.1.4	Software Programs and Data Analysis	49
5.2	Results	49
5.2.1	Velocity Results	49
5.2.2	Laser Results	50
5.2.3	Consistency	51
6	Conclusions and Future Work	53
6.1	Conclusions	53
6.2	Future Work	53
6.2.1	Improvements to Air Flow and Rig	53
6.2.2	Improvements to Testing Section	54
6.2.3	Improvements to Analysis and Software	55

<i>CONTENTS</i>	xi
7 Abbreviations	57
A Figures	59
B Tables	83
B.1	83
C Equations	85
Bibliography	85



List of Figures

1.1	Timeline of Project	3
2.1	Effect of Inhalation flow on %FPF on an example combination of DPI and Formula [1]	6
2.2	Representation of DPI's Stages [2]	8
2.3	Sample Version of How D values are Calculated [3]	10
3.1	Box Diagram of the DPI rig setup	18
3.2	Engineering Sketches of New Testing Section	20
3.3	Assembled Rig	26
3.4	Disassembled DPI Rig	27
3.5	Initial Testing Section Assembled	28
3.6	Assembled Hotwire	29
3.7	Assembled Laser Diode Pointer	30
3.8	Assembled HeNe Laser	31
3.9	Raw Data vs Filtered Data	32
3.10	Basic Diagram of How The Laser is Affected by Particles	34
3.11	Where origin is	34
4.1	Volume Flow Rate vs Velocity of Averaged Values for Varying Pressures from Table 4.1	36
4.2	Volume Flow Rate vs Velocity of Averaged Values for Varying Pressures from Table 4.2	37
4.3	Volume Flow Rate vs Velocity of Averaged Values at 100kPa from Table 4.3	37
4.4	control tests between diode and HeNe laser	38
4.5	Comparison of Different Sample Rates and Time	40
4.5	Different height going towards flow at 2mm increments	42
4.6	Different height going away from the flow at 2mm increments	43
4.7	Tests at pocket 2mm towards	44
4.8	SV010 through pocket 2.5mm down adn 15mm towards flow	45
5.1	Powders left in Pocket after 5 seconds	52
A.0	Risk Assessment of Project	61

A.0 Engineering Sketches of the Dry Powder Inhaler Rig	65
A.1 Overview of Remodeled Parts	66
A.2 Photodiode Specifications [4]	67
A.3 LABVIEW inputs and Setup	68
A.4 Hot Wire Anemometer Specifications [5]	69
A.5 Transistor Specifications	70
A.6 HeNe laser Specifications [6]	71
A.7 Pressure Regulator Specifications [7]	71
A.8 Flow Meter Specifications [8]	71
A.9 Sample MATLAB Code	71
A.10 Raw and Raw Vs Filtered Data	72
A.11 Raw and Raw Vs Filtered Data	73
A.12 Raw and Raw Vs Filtered Data	74
A.13 Raw and Raw Vs Filtered Data	75
A.14 Raw and Raw Vs Filtered Data	76
A.15 Raw and Raw Vs Filtered Data	77
A.16 Raw and Raw Vs Filtered Data	78
A.17 Raw and Raw Vs Filtered Data	79
A.18 Raw and Raw Vs Filtered Data	80
A.19 Attendance With Supervisor	81

List of Tables

2.1	Current Techniques Used for Research on DPIs and their Purpose	11
3.1	Theoretical Calculations for Velocity, Volume Flow and Reynolds Number for Boundary Flow For a Given Reynolds Number Pipe Flow	19
3.2	Equipment that will be organised by the supervisor and university	21
3.3	Equipment that has been organised by the author include	22
3.4	Powders and their Specifications	23
3.5	Parts and the reasonings for the obtainment	24
4.1	Averaged Values for Hotwire Testing With The Pocket Attached	35
4.2	Averaged Values for Hotwire Testing With Solenoid Attached	35
4.3	Averaged Values for Hotwire Testing at 100kPa	36
4.4	Largest ST.DEV of each Test	36
4.5	Comparison of powders from Figure 4.7(a)	45
4.6	Comparison of powders from Figure 4.7(b)	45
4.7	Consistency tests using SV010 2.5mm down and 15 mm towards flow from origin	46
B.1	Properties Used in Theoretical Calculations	83
B.2	Kolmogrov's Length, Time and Velocity Scale	84



Chapter 1

Introduction

Asthma affects 10.8% [9] of the Australian population, while Chronic Obstructive Pulmonary Disease (COPD) affects 14% [10] of australians over 40 (COPD is mainly diagnosed for patients over 40 years of age [10]). While Asthma and COPD are at their base different, they share common symptoms and treatments which come in the form of injections, tablets, nebulizers and inhalers. Inhalers come in two distinct categories, Metered Dose Inhalers (MDIs) and Dry Powder Inhalers (DPIs). DPIs have become increasingly popular devices due to their user friendly nature. This is due to DPIs working off the patient's own inhalation profile at their own pace, unlike MDIs where there is a need to sync breathing with the release of chemicals evacuating from the chamber. This however creates complications as the effectiveness of the device is significantly impacted upon by each patient's inhalation profile, making them a poor choice for those with low inhalation flows such as children, the elderly and those with restricted breath as a result of suffering an attack.

To contend with these problems, research institutes and pharmaceutical companies such as DFE Pharma have been researching into the current designs of the devices, physicochemical properties of the formulations, the effect of the airflow inside the devices and new innovative designs to improve current knowledge. This will hopefully enable the design of a more efficient device as well as the ability to create DPIs that can cater to different inhalation profiles.

This project looks into the proof of concept and analyses initial stages of results for a project that will be continued on after this. The project requires the redesign of a previous experiment to obtain repeatable tests procedures, acquisition of required parts and assembly of these into a functioning experiment. Initial experiments will be used as a base for further experimentation to work upon, by supplying validation and basic understandings and results of what will happen.

It is currently known that turbulence can increase the aerosolisation of particles and help with the deagglomeration. [11, 12], However it is not known to what degree and at what rates of turbulence can actively increase the overall performance. The project focuses on a systematic study of the effect of Reynolds numbers on the particle flow in simple geometries where the boundary conditions are well defined. This also allows for the

development of data sets that can be used for validation in computational fluid dynamic models. In combination with the use of advanced laser diagnostic techniques that have seldom been applied to such a problem, the discoveries made in this project are expected to have a significant impact on the current understanding of dry powder inhaler flows.

This will be done by investigating how different sized particles are affected by different local velocity conditions, through a systematic control of the Reynolds number. The use of laser diagnostic equipment will allow for non-invasive measurements for shear forces, natural forces and evacuation times of designated areas. The aim is to advance the current knowledge of particle flow in order to allow both research institutes and pharmaceutical companies to be able to target powder properties and inhaler designs to different inhalation profiles, minimizing drug wastage and cost.

1.1 Objectives

The main objectives of this project were to redesign, acquire, assemble and provide initial tests of a unique rig to prove and find problems with the concept. These will be achieved through

- A write up of theoretical results for expected velocities and volume flow rate for different Reynolds rates the redesign of a previously established experiment
- To locate and obtain parts to address redesign
- Assemble the redesigned Rig
- Test performance of the rig
- Test produced velocity readings
- Take initial laser readings
- Obtain results where possible

1.2 Limitations

1.2.1 Time

Due to the time constraints of a semester, limitations were put on the parts used, the amount of time available for testing and the different types of testing. This meant that Parts that may have been a more suitable for this project were overlooked for parts that were readily available. While the limit on Time meant testing with the HeNe laser was shortened due to the need for a supervisor and that the normal section was never finished and no tests were taken for it.

1.2.2 Cost

Costs also placed a limitation the parts available, as there was a grant of roughly \$600, limiting the spending of parts, such as the ball rotameter.

1.2.3 Materials

The powders used had an expiry date where, once reached they no longer have the same properties that they are generally attributed. This was seen to happen with SV 004 where it was no longer available to work with as it had become clumpy due to an increase in moisture content.

1.3 Project plan

	Jun	Jul	Aug	Sep	Oct	Nov
Task 1						
Task 2						
Task 3						
Task 4						
Task 5						
Task 6						
Task 7						
Task 8						
Task 9						
Task 10						

Figure 1.1: Timeline of Project

1. Obtaining Permissions and training for use of labs
2. Design changes to original plans
3. Perform Calculations
4. Obtaining required parts
5. Assembly of equipment
6. Testing of equipment
7. Hot wire testing
8. Assembly of laser pointer

9. Laser pointer measurements
10. Write up

1.4 Risk Assessment

A risk assesment was conducted and can be seen in Figure A.0

Chapter 2

Background and Related Work

2.1 Introduction

With the increase in interest of DPIs, there has been a significant shift in research towards making a more efficient inhaler. Research is headed primarily towards improving the design of the device and the developing physicochemical properties of the formulation. Research is also being done for expanding the use of inhalers in applications outside of Asthma and COPD. This has driven the investigation into targeting different inhalation profiles, targeting specific parts of the lungs and catering to patients preference. These advancements will allow for inhalers to be used in other areas such as a pulmonary vaccination and the decrease of fine particle fraction (FPF) variations between patients. Through improved targeting of the aggravated areas, DPIs will provide faster and superior relief and also minimize drug wastage. These advancements along with the continual improvement of computational fluid dynamics (CFD) in conjunction with the discrete element method (DEM) and advanced technologies show a bright future for DPIs.

2.1.1 Importance

Inhalers have become an important aspect in many people's lives as they can provide quick relief and prevention to pulmonary tract infections such as asthma and COPD. This can be seen in the Australian Health Survey: First Results from 2014-15 that found in Australia alone it was reported that 10.8% [9] of the population have been recorded with asthma while COPD is the third leading cause of death worldwide in 2010. [13].

This is further backed up by a study from the Australian Institute of Health and Welfare where it was found that there were 12,553,247 prescriptions for respiratory medication in 2013, which does not even include over the counter products [14]. MDIs have been the most commonly used inhalers for roughly the last fifty years, however as explained by Newman [15], there are limitations such as the patient's inhalation technique, the risk of inducing bronchospasm and the production of extensive oropharyngeal deposition. But more noticeably, the banning of use of Chlorofluorocarbons as a propellant, due to its damaging properties to the ozone layer. This has led to different propellants to

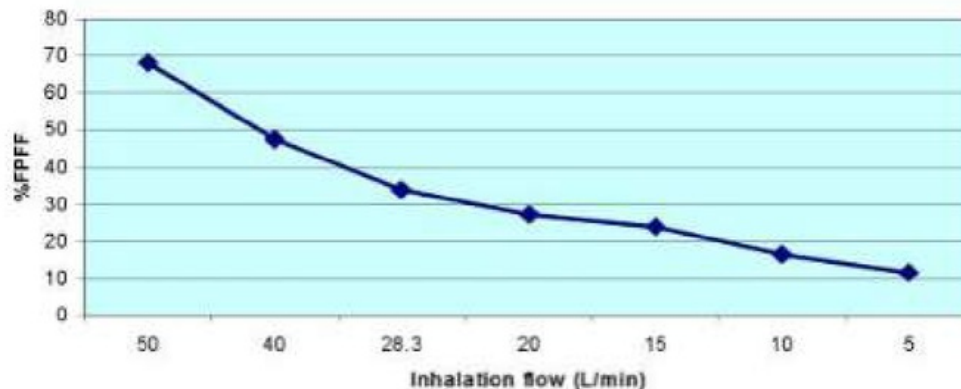


Figure 2.1: Effect of Inhalation flow on %FPF on an example combination of DPI and Formula [1]

be used such as hydrofluoroalkanes which are also known to be detrimental to the environment [15, 16]. DPIs have thus become an interesting alternative as they are relatively easy to use in comparison to MDIs and require no propellants, relying on the patient's own air flow instead. While this is one of its most useful properties, it also is one of its most limiting factors, due to the large differences in inhalation profiles, leading to varying degrees of FPF that are actually delivered to the lungs seen in Figure 2.1 and in Cleary et al. [1, 2, 11, 16–19].

There has also been an increase in research for the use of DPIs in areas other than Asthma and COPD. Telko and Hickey [18] discuss the new avenues of research, such as the use of antibiotics against infectious diseases originating from the lungs like cystic fibrosis, systemically acting drugs such as insulin for diabetes and as vaccination programmes against viral disease like influenza. This expansion in applications of DPIs is also expressed by Hoppentocht et al. [16] discussing the use as a pulmonary vaccination.

2.1.2 Chronic Airway Disease

Asthma and COPD are the main contributors to Chronic Airways Disease. While Asthma and COPD have separate sources, they impart similar symptoms that can be treated in the same way. These symptoms for Asthma and COPD include wheezing, coughing, difficulty breathing, tightness in the chest and shortness of breath.

Asthma is a long term lung condition that is not fully understood but is believed to be caused by a combination of environmental and genetic factors. Asthmatics have sensitive airways in their lungs that are prone to triggers resulting in flare ups that constricts the muscles, thus squeezing the airways tight. The airways then swell becoming narrow and producing more mucus making breathing difficult [20]. These triggers can be due to allergens, irritants in air, extreme changes in weather and exercise or illness.

Asthma has three major components to it being Inflammation, Airway hyperresponsiveness and Bronchoconstriction.

- Inflammation causes swollen airways and excess mucus which causes a reduction of size in the airways. This can be consistently present, not just during an attack.
- Airway Hyperresponsiveness alludes to the airways of asthmatics being extremely sensitive to certain changes.
- Bronchoconstriction is where the muscles lining the airways constrict squeezing the airway and narrowing the passage for air flow when triggered [21].

COPD however is a progressive condition that mainly affects older people and is distinguished by airflow limitation that is not completely reversible. The main cause being smoking or exposure to smoking [10]. COPD covers a variety of lung diseases including emphysema, chronic bronchitis and chronic asthma. Similar to Asthma the symptoms include losing breath easily, a new or persistent cough and a buildup of phlegm. These symptoms however are a result of damage to the air passages in the lungs. The Bronchial tubes become narrower, lungs are larger than normal, so the breathing muscles around the outside of the lungs become stretched and have to work harder, making breathing harder and causing smaller breaths.

Treatment

Treatment of these diseases come in the form of injections, tablets, nebulizers and inhalers. These treatments can be categorised as

- Short Acting Bronchodilators (beta agonists (SABA) or anticholinergics/muscarinic antagonist(SAMA))
Are used as relievers as they provide quick relief, in opening the airways to make breathing easier. Used in inhalers or liquid form to be used in nebulizers
- Long acting bronchodilators (beta agonists (LABA) anticholinergics/muscarinic antagonist (LAMA))
Are used as preventers that combat the symptoms over time, needing daily use to provide less contracted airways and desensitization to triggers
- Corticosteroids (ICS inhaled corticosteroids)
Used to reduce inflammation in the body (sufferers can have inflamed airways). It can be used as both preventer as an inhaler or liquid or used in emergencies as a pill, liquid or as a shot, depending on the type.
- Phosphodiesterase-4 inhibitors
Helps relieve inflammation as a reliever alongside bronchodilators as a pill

- Methylxanthines

For cases with severe COPD this is prescribed as a pill or liquid to be used in conjunction with bronchodilators as an anti inflammatory

[22]

2.2 Dry Powder Inhalers

Dry Powder Inhalers are devices that deliver medication to the lungs through the use of the users own inhalation in the form of a dry powder. DPIs go through four main stages entrainment (otherwise known as aerosolisation or fluidisation), deagglomeration of the active drug particle, transportation of the drug aerosols through the airways and deposition [2, 11, 16, 17, 19]. This can be seen in Figure 2.2.

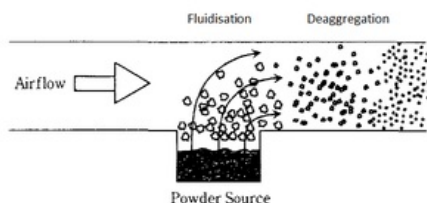


Figure 2.2: Representation of DPI's Stages [2]

When the DPI is actuated, the formulation is released from its container and is then entrained, which is the process of lifting the powders into the air flow. The next stage is deagglomeration, being the act of breaking apart the clumps of powder that has agglomerated (clumping into balls) to adequate sized particles through fluid and or impact forces. These fluid forces incorporate fluid shear forces, sudden accelerations from drag forces, as the flow has varying velocities. The impact forces can occur from impaction upon other particles, or purposely built geometries. At this stage, for powders using carrier particles, the Active Pharmaceutical Ingredients (API) are detached from the carriers and are dispersed, where the carriers should remain in the upper airways while the FPF travel through the mouth and are deposited into the alveolar region of the lungs. [2, 11, 16, 17, 19]

DPIs have many variations in form which is one of the reasons why it is impossible to create overarching predictions of how well they work. One such category involves the dosing system which can includes a single dose unit using a capsule that is disposable, a multi dose unit, that has a pre metered unit with replaceable set and a multiple dose reservoir. [11] For further knowledge on different categories used and dry powders available Kou and Cao provide a brief summary of current devices and highlight some new developments [23]

2.2.1 Entrainment

Entrainment is the act of sweeping up the powder through use of the air being inhaled. This is achieved separately for each unique device but can be simplified by thinking of a particle that is attached to a plane wall through adhesion. As a flow comes through, the fluid exerts a vertical force on the particle overcoming the adhesive force and weight of the particle. This is most common method used in DPIs being shear fluidisation, called this due to the strong shear force that occurs near the boundary layer due to its thin nature. Other entrainment mechanisms include gas-assist, capillary, mechanical and saltation. [2, 12]

Entrainment is the act of sweeping up the powder through use of the air being inhaled. This is achieved separately for each unique device but can be simplified by thinking of a particle that is attached to a plane wall through adhesion. As a flow comes through, the fluid exerts a vertical force on the particle overcoming the adhesive force and weight of the particle. This is most common method used in DPIs being shear fluidisation, called this due to the strong shear force that occurs near the boundary layer due to its thin nature. Other entrainment mechanisms include gas-assist, capillary, mechanical and saltation. [12, 24]

2.2.2 Carriers

Carriers are an important part of DPIs formulation as they are known to increase the efficiency. Carriers are implemented as bonds made between the carriers and APIs are significantly weaker than those formed between APIs making the force needed for deagglomeration and dispersion significantly lower. Carriers are also known to make entrainment easier as their larger size exposes them to significantly higher lift forces exerted upon them [11, 12].

The majority of carriers are Lactose based due to their versatility. Lactose normally used in DPIs include sieved lactose, milled lactose, spray dried lactose, granulated lactose and anhydrous lactose [25]. It should be noted that milled lactose has a higher accuracy of targeted particle size than sieved [25]. However there has been research into the use of alternative sugars such as sorbitol, mannitol, glucose, maltitol, xylitol and trehalose to name a few [11]. This can be seen in Minee et al. studies the influence of formulation carriers of physical characteristics of inhalation and in Teckel and Bolzen search of alternative sugars as a potential that found mannitol as a potential drug carrier over more hygroscopic sugars that had poor dispersibility.

2.2.3 Particle Size

Particle size is mainly discussed as particle size distributions known as D values. The D values are D10, D50 and D90 which represent the ranges of particle sizes of a given sample. Traditionally done by creating an S-curve of cumulative mass retained against a sieve and calculating the intercepts for 10%, 50% and 90% mass. This is seen in Figure 2.3 [3]. Particle Sizes are extremely important as knowing dimensions of particles

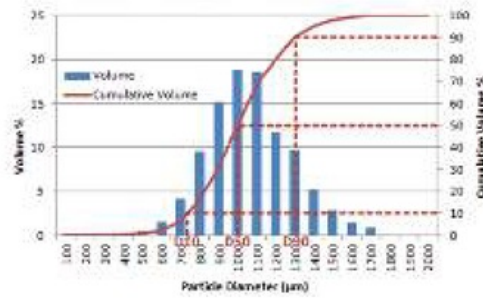


Figure 2.3: Sample Version of How D values are Calculated [3]

can help to predict the flows and is a determining factor in how the particle will react in different environments. For example FPFs are designated to be less than $5\ \mu$ [16, 26, 27] and is used as a basis for the size of particles that will reach deep into the lungs.

2.3 Current Research Techniques

Research is currently improving through the use of CFD and DEM which is discussed and used in [2, 11, 16, 18, 26, 28–32]. These tools are extremely useful as they can simulate the particle flow however are dependant on experimental correlations and the user's input. This results in the need for them to be used in conjunction with real world experimental testing to validate the models. These can include

[2, 11, 16, 18, 27, 28]. The majority of research has been done by designing and creating unique equipment setups involving these techniques. CFD and DEM analysis are widely used in conjunction with the techniques seen in Table 2.1 to validate the analysis provided from the Computation analysis. [11, 27, 28, 33]

2.4 Current Research

Islam & Cleary [11], Islam & Gladki [17], Dunber et al. [2], Newman & Busse [34], Hoppentocht et al. [16] and Dal [19] all provide a review of current DPIs technology and the direction that it is expected to take. In each study there is a concurrence that while DPIs have great potential, they state there are still major limitations that need to be overcome such as the efficiency of the DPIs and the inter and intra-patient variability of the FPF that reach deep into the lungs. It is also agreed that advancements in designs of the device go along with the physicochemical properties being dependant on each other. [2, 11, 16, 26, 31, 34, 35]

Technique	Purpose
CFD	Used to Simulate Fluid Flow
DEM	Used to simulate the motion of large numbers of particles
Annular Shear Testing	
Scanning Electron Microscopy	Visualisation of formulation and agglomeration geometry
Atomic Force Microscopy	Determines the single contact point adhesive forces between individual particles
Inverse Gas Chromatography	Determines surface energy characteristics of bulk formulations
X-ray Diffraction	Determines crystal structure and formulation composition
High Speed Photography	Direct Visualisation
High Speed Photography with Laser Diffraction	Allows for particle size distribution in real time while entrained
Particle Image Velocimetry	Determines air velocity and related quantities
Laser Doppler Velocimetry (LDV)	Determines air velocity and related quantities
Multi Stage Liquid Impingers	Determines particle sizes, particularly when determining FPFs
Cascade Impactors	Determines particle size

Table 2.1: Current Techniques Used for Research on DPIs and their Purpose

2.4.1 Design of Device

One avenue of research that is being undertaken to improve the reliability of DPIs is the design of the device. Reviews on the designs of devices can be found in [2, 11, 16, 17, 19, 23, 34, 36].

Dal [19] states that an ideal device needs to be:

- Effective
Is able to deposit the a sufficient amount of the drug to desired location, independant of the users inhalation profile
- Reproducible
This is repeatable
- Precise
Able to know the amount of drug/doses remaining and if the procedure was performed correctly
- Stable
Able to protect the formulation from environmental changes
- Comfortable
Easy to understand and use, particularly in dire conditions
- Versatile
Able to use other drug formulations
- Environmentally compatible
Does not use or contain chemical contaminants that may harm the environment
- Affordable
Has an acceptable cost with the possibility of being able to recharge the dose/s.

While current DPIs are a long way off these ideal standards, through continued research they are improving at a significant rate. However majority of research on the device of the design is in improving the efficiency of DPIs.

Coates et al. [29] studied the effect of modifying the design of a DPI (Aerolizer® in this case), by varying the inhaler grid and mouthpiece length. This is done through the use of CFD and validated through LDV and a multistage liquid impinger using mannitol powder at 60 l/min . The results showed that with increased grid voidage, device retention increased which lead to a decrease in FPF, however the length of the mouthpiece had no significant effect on the flowfield. This is an important study as it found that simple design changes can affect the performance of the DPIs.

Continuing on from Coates et al. [29], Coates et al. [30] studies the effect of the change in air inlet size, specifically the flowfield generated in the device and the resistance from

the device and subsequent effect on deagglomeration. This is again done through the use of CFD and validated with a multi-stage liquid impinger with a mannitol powder based on an Aerolizer®. The tests used three different inlet sizes resulting in 30, 45 and 60 l/min flows. These results found that at low flow rates reducing air inlet size increased dispersion performance while at higher flow rates it lowered it. This is interesting as it portrayed that maximum inhaler dispersion performances can be predicted if the devices flowfield is known and the effect of changing the inlet size and therefore volume rate affects the overall performance of the DPI.

A later study by Coates et al. [26] continues to take an indepth look at the devices specifically into how the geometry of the mouthpiece affects throat deposition, device retention and the performance of the delivery rate of FPF. This Research paper uses CFD analysis on the flowfield that is generated in an Aerolizer® and validates it with experimental dispersions of a mannitol powder for modified mouthpieces including cylindrical, conical and oval designs. The results found that it had no effect on the overall performance and device retention but had a significant effect on throat deposition. This research is important as it seeks to understand the effects of mouthpieces and how it can be applied to improve the efficiency of DPIs. This is because the reduction of throat deposition is linked to the total amount of FPF reaching the lungs, while decreasing device retention reduces the amount of drug wasted inside the device, and thus entering the user.

Srichana et al. [35] looks into the effect of resistance of devices and the influence of powder formulation on the deposition of the carrier. This was done by measuring the pressure drop across the devices and measuring the FPF of multiple devices with varying formulas over different flow rates. The research performed tests on the Ingelheim®, cyclohaler®, Rotahaler®, Spinhaler® and Diskhaler®. Its findings show that with higher resistance devices there was greater FPF, however this changes when the use of the formulations that is created in combination with the device is used. This is important as it shows that the combination of device and formula is currently needed to create an efficient DPI.

Donovan et al. [31] investigates the influence different DPI designs have on the effectiveness of carrier particles. CFD is used in conjunction with a through a cascade impactor at 60l/min, on the Aerolizer® and Handihaler® with lactose ranging up to 300µm. The results found that an increase in carrier sizes increased carrier deposition in the aerolizer, while they were found to be less frequent in the handihaler and mostly independent of the particle size. This is an important step as it shows that the behaviour of carrier particles is not only influenced through the physicochemical makeup but the devices design.

These articles show the increasing prevalence of research to not only focus on the design of the device but a combination of the design and physicochemical properties.

2.4.2 Physicochemical Properties and Morphology

Physicochemical properties are another significant avenue of research along with device design. Reviews on the designs of devices can be found in [2, 11, 16, 17, 34, 36]. Telko and hickey [18], expanding upon the the challenges and areas involved with the physic-

ochemical properties. This includes how the powders act differently when in different states i.e. static powders behave as solids, when flowing like liquids and when dispersed in air conforms to its carrier gas. This poses a problem for accurate predictions as the equations used rely on empirical and/or assumptions of approximates due to differences in each particle.

Research into the physicochemical properties and morphology of can be seen in Kawashima et al. [37], Telko & Hickey [18] and Le et al. [38].

Kawashima et al. [37] investigates the effect of surface morphology of carrier lactose on the properties of the SABA/SAMA Pranlukast Hydrate. This is completed by mixing it with pharmatose 325M, 200M, DCL-11, DCL-21, spray dried amorphous, spray dried crystallized lactoses and fluidised bed granulated lactose with various surface morphologies. This is then put through a Spinhaler® and evaluated by a twin impinger. As a result it was established that carriers with large surface areas with microscopically increased surface roughness was also able to improve efficiency thus portraying how the separation of the API from the carrier is an important step to improve the efficiency of DPIs.

Telko and Hickeys [36] research is based on the variables of the formulation of aerodynamic and electrostatic properties. This was done using Albuterol and Budesonide with a combinations of different carriers, concentrations, doses, metering system and flow conditions. To evaluate the results the samples were collected in an electrical low-pressure impactor and eight stage cascade impactor allowing for the calculation of the approximate aerodynamic particle size distribution and particle charge levels per particle. The results found that charge levels were considerably higher than previously estimated by orders of magnitude higher than predicted by the Boltzmann charge distribution. Further proving the challenge that is undertaken when trying to predict particles.

Le et al. [38] studies the parameters of carriers and APIs in adhesive mixtures used in DPI and their effect on dispersion. This is carried out by mixing Fluticasone Propionate with Lactohale 200, with variations of operating conditions being speed, mixing time, resting steps during mixing, the size of the carrier and storage conditions. The adhesion characteristics were evaluated through sieving while the FPF was done through a twin stage impinger. The results show that for a good dispersion the speed and powder blending have to be sufficient without going on for too long to prevent the appearance of static electricity while there is an increase of FPF was found when the carrier size was decreased and there was lower humidity. This is an important step as it provides a basis of understanding in the manufacturing of the formulations.

The research on physicochemical properties and morphology shows that it is an extremely interesting but challenging area, where sound hypothesis may not work out as expected.

2.4.3 Effect of Air Flow

Coates et al. [32] and Behara et al. [39] both study the effect of air flow within a DPI but for different purposes.

Coates et al. [32] investigates influence of airflow on the overall performance of DPIs and initial quantification of turbulence levels and particle impaction velocities the maximised performance. This was accomplished by using CFD in conjunction with a multistage liquid impinger using a mannitol powder based on an Aerolizer® over different flow rates. This found that both powder dispersion and throat dispersion increased with air flow while capsule retention lowered and device retention first increased and then decreased. These multiple variables lead to an optimal performance at 65 l/min and correlations between the flow rate, throat deposition and capsule emptying times. This is particularly important for this project as it has similar themes however unlike Coates et al. [32] which has a targeted view on the Aerolizer®, this project will be aiming to cover simple geometries that will be able to be used in many different areas.

Behara et al. [39] studied the effect of three commercial DPIs and their sensitivity to air flow rate changes and air flow resistances. This project was based on the three devices, Rotahaler®, Monodose Inhaler® and Hanihaler® with Salbutamol Sulphate and LH300 as the formulation. The aerosolisation was assessed using the laser diffraction method between flow rates of 30 to 180 l/min. The findings portrayed that the relative deagglomeration between devices was substantially different. This reinforces prior research that different devices behave contrastingly with the same formulation and how a new approach can lead to discoveries.

The investigation into the airflow is an extremely important aspect of DPIs but as seen in this section that it is a very narrowed focus on pre existing DPIs with minor changes.

2.4.4 Patient Training

Patient training is considered to have a significant effect on the efficiency. This is seen in Lavorini et al. [40] study where depending on which inhaler was used 40% of patients are using their inhaler incorrectly leading to a drop in efficiency. This is seen in Chrystyn et al. [41] which tested patients ability to adapt to using a new DPI. The need for patient training and device designs that are practical and easy to use, is also discussed in Islam and Cleary [11] where the variability between patients is a major issue.

2.4.5 New Novel Devices

Islam & Gladeki [17] show an in depth approach to whether optimising existing devices (such as the Rotahaler®, Turbuhaler®, Easyhaler® and Spinhaler®) is more important than research into new novel devices. By doing this they are weighing the consequences of stability of known working products and innovation. Their finding proved that both optimising and innovation of new devices is equally needed.

One new Device is a High Dose DPI based on a fluidised bed which was designed by Farkas et al. [42]. This device implements a similar concept to fluidised beds for

aerosolisation using small mixing balls, along with larger hollow dosing spheres filled with powder and was compared to other capsule based DPIs through emitted dose and aerosolisation efficiency. It was found that it was improved with the removal of the mixing balls while still maintaining its efficiency.

Other improvements are seen through active DPIs that are power driven helping with the airflow such as having a bolus of compressed air that releases with the powder when breathed in [2, 11, 17]. These active devices that are power assisted (whether it is pneumatic, impact force or vibratory), are not subject to the same limitations as the normal passive inhalers, and have been suggested if shear and turbulence could be standardised through a dispersion mechanism independent of a user's breath could create an efficient DPI that is not restricted to the users inhalation profile [18].

2.5 Conclusion

DPIs are a source of substantial potential to many suffers of Asthma and COPD due to their relative ease of use and lack of propellant that can damage the environment. There are still significant limitations that need to be overcome to allow DPIs to meet standards such as the efficiency levels of FPF reaching deep into the lungs and the variations occurring per patient. This however is being addressed through the research combining advanced technological techniques, CFD and DEM, into the design of the devices, the physicochemical properties of the particles, correct training of patients and new innovations.

Chapter 3

Approach and Testing

3.1 Introduction

The original experiment was designed by a previous Master's student but was abandoned and picked up as an undergraduate thesis. Due to the change in researchers and circumstances, the approach has been remodeled to further suit the objectives that have been set, this will be explained further into this paper. Theoretical results will be obtained to get an understanding of the expected velocities and flow rates needed to get a range of laminar to turbulent flows

The rig will use air supplied from the laboratory taps that will be constrained to a set pressure and volume flow, which will then be held by a solenoid valve for precise control, to flow into the rig where the air will interact with the powder through shear forces. The use of a hot wire will be used to validate the expected velocities going through the rig, while a non-invasive measurement involving a laser and a photodiode will be used to gather data. Seen Figure 3.1

Once testing commenced it will be done using the previously mentioned powders in Table 3.4, Ideally the pressure used would have centered around 100-200 kPa and covered a range between 50-400 kPa, this would have then been further changed in accordance to the Reynolds number of the flow over 1000-10000 and thus covering laminar to turbulent flow. However due to size of the pocket, aerosolisation only occurs at 70 l/m and above. This posed a problem as the solenoid valve only goes up to 60 l/m for pressures at 100 kPa, thus tests have been done at 300 kPa and 80 l/m to ensure decent aerosolisation occurs. Once the new powder test region is created it will slip into where the original piece was and will continue to act in a similar manner, however access to the interior will be through the top that can be screwed down.

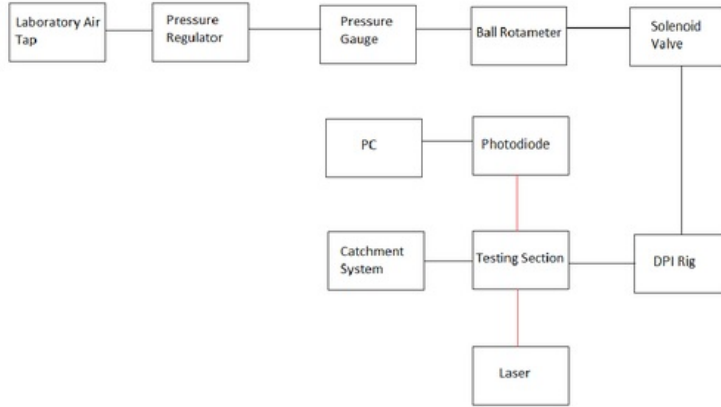


Figure 3.1: Box Diagram of the DPI rig setup

3.1.1 Theoretical Calculations

Equations used for Table 3.1 are shown below in Equation 3.1, Equation 3.2 and Equation 3.3

$$u = \frac{Re_{pipe} * v}{d_h} \quad (3.1)$$

u = Velocity, Re = Reynolds Number in Pipe Flow, v = Kinematic Viscosity, d_h = Hydraulic Diameter

$$Q = u * A \quad (3.2)$$

Q = Volume Flow Rate, u = Velocity, A = Area

$$Re_{bound} = \frac{U_{\infty} * x}{v} \quad (3.3)$$

Re_{bound} = Reynolds Number in Boundary Layer, U_{∞} = Free Stream Velocity, x = Development Length, v = Kinematic Viscosity

Reynolds number for pipe flow enters the transitional phase at 4000 and is truly turbulent at 7000, while the Reynolds number for Boundary layer is laminar for $<10^5$ and turbulent for $>10^6$. Values used in Equation 3.1, Equation 3.2 and Equation 3.3 are found in Table B.1

Table 3.1 shows the theoretical calculations to have a range of fully laminar to fully turbulent for both flow in a pipe and boundary layer. The calculations show that there will be expected velocities between 1-10 m/s needed that is driven by a flow rate of 13.6 l/m to 136 l/m.

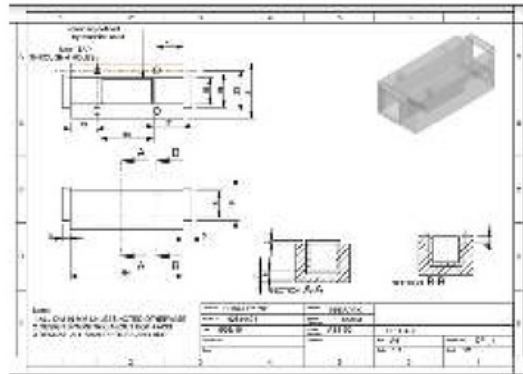
Reynolds Number Pipe Flow	Velocity (m/s)	Volume Flow (l/m)	Reynolds Number Boundary Layer
1000	1.007	13.599	14000
2000	2.015	27.198	28000
3000	3.022	40.797	42000
4000	4.029	54.396	56000
5000	5.037	67.995	70000
6000	6.044	81.594	84000
7000	7.051	95.193	98000
8000	8.059	108.792	112000
9000	9.066	122.391	126000
10000	10.073	135.99	140000

Table 3.1: Theoretical Calculations for Velocity, Volume Flow and Reynolds Number for Boundary Flow For a Given Reynolds Number Pipe Flow

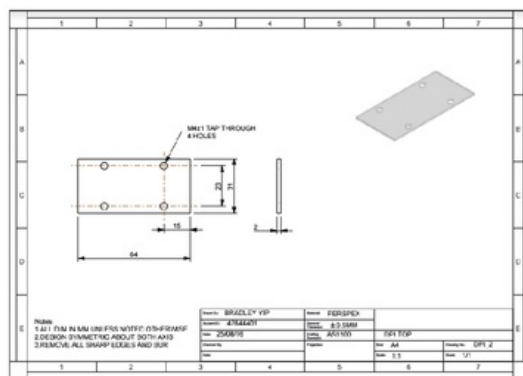
Further Calculations were done for those interested on the kolmogorov scales signifying the smallest eddy length, velocities and times. Seen in Table B.2

3.2 Parts

Equipment will reside at Macquarie University in E6A lab 218. Equipment that will be organised by the supervisor and university includes.



(a) New Section Pt.1



(b) New Section Pt.2

Figure 3.2: Engineering Sketches of New Testing Section

Part	Specification
THOR Honeycomb Optical Breadboard	M6 holes spaced 25mm apart
Pole Stands	M6 threaded
Boss Head Clamps	
Three Prong lab clamp	
Optical Base Plates	
Optical Posts	M6
Optical Railing	Scale in mm
Electrical Breadboard	
Air Taps	Supplies compressed air between 700-800kPa
Pressure Gauge	Reads between 0-400 kPa
Dry Powder Inhaler Rig	made in mets seen in Figure A.0, however changes have been made to the base plate with five extra holes drilled into it seen in Figure A.1(a)
Photodiode SD 112-42-11-221	seen in Figure A.2
Data Acquisition Board (DAQ board)	
National Instruments NI cDAQ-9174	four slot USB chassis, supports analog, digital, inputs and outputs up to 1 MHz, for more see [43]
(DAQ board) attachments NI 9223	four channels, range $\pm 10V$, sample rate of 1 Million Samples/s for more see [44]
(DAQ board) attachments NI 9401	eight channels, update rate is 100 ns for more see [45]
PC with Labview and national Instruments drivers installed	see Figure A.3
Hot-wire DT-8880	see in Figure A.4
Hose clamps	Able to clamp over a 15 mm dia
Screws, Nuts and Bolts	M6 NPT
Hydraulic Fitting T Section	1/4" BSP
Hydraulic Hosetail/Male-BSP	3/8", 1/4" BSP
Electrical Breadboard	
DC Power supply	0-20V
Teflon Tape	
Electrical Wires	
2N3773 Transistor	See Figure A.5
Resistor	100 Ohms
Red Helium-Neon laser R-30990	seen in Figure A.6
Hand held Vacuum Cleaner	

Table 3.2: Equipment that will be organised by the supervisor and university

Part	Specification
SMC AR20-02-B Pressure regulator	Seen in Figure A.7 \$52.95
Flowmeter, MR3A18BLBN	Seen in Figure A.8 \$130.61
Two Red Laser Diode Pointer	Battery powered, 630-680nm, Output <1mW, \$15 ea
Hose Air Application Tube	dia 12mm, length 20m, \$49
2x Hex Nipple	1/4" BSP \$2.18 ea
2x Hosetail/Male-NPT	3/8", 1/8" NPT \$3.30
BACOENG DC12V electric Solenoid valve	1/4" BSP, DC12V, Brass, Normally closed, Suitable for water,oil or air, Working pressure: 0-1 Mpa, \$47.87
RS Pro, male BNC to Crocodile Clip	1m, 50 Ohms impedance, \$11.27
New Powder Test Section	Designed and made in METS, seen in Figure 3.2
Catchment System	Small catchment device built

Table 3.3: Equipment that has been organised by the author include

3.2.1 Materials

Part	Specification
Powder Respirator SV004	Coarse Sieved D10 within 5-10 m is 6 m
Powder Respirator SV010	Coarse Sieved D10 within 35-65 m is 51 m
Powder Lactohale(LH) 200	Milled D10 within 5-15 m
Powder Lactohale(LH) 206	Milled D10 is 38 m

Table 3.4: Powders and their Specifications

3.2.2 Reason for Selection

Seen in Table ??

3.3 Assembling of Equipment

This investigation had five major components that combine together to produce the results. The components being the remodelling and acquisition of parts, acquiring and control of the airflow coming into the the DPI Rig, The DPI rig itself, the testing components and the Data analysis. All connections were either clamped or covered in teflon tape to ensure that there were no leaks within the system and used BSP fittings unless mentioned otherwise.

3.3.1 Remodeled Sections

Problems occurred with original design featuring the connection of the base plate to the optical breadboard, the testing section and the swivel based loading system. The bracing of the support plates holes were not designed to match up with the optical breadboard and required four outer holes 25mm in in each corner to allow for it to be compatible with the optical breadboard and an extra hole underneath the testing section to allow for a bolt to be screwed to the base allowing it to be moved up and down to ensure the pocket is flush against the section This is seen in Figure A.1. The testing section that was made and seen in Figure A.1(j) had incorrect dimensions as it is 2 mm longer than the pocket, thus leaving a major leak that was rectified by breaking off one of the lower bracings and re gluing it into place to ensure airtightness, this however was only a quick fix and a new testing section was designed and implemented to ensure there was no leaks and problems seen in Figure 3.2.

The swivel loading system was attempted however it was ultimately scrapped as it produced to many problems and was not a viable option. This was due to the swivel not being able to spin freely due to supports being in the way and the pocket not fitting into the testing section without sliding it in. This was rectified by separating one of the

Part	Reason
Fittings & Screws	Nuts and bolts are all M6 unless expressed otherwise, this is to be compatible with optical breadboard, Hydraulic fitting are all BSP unless mentioned otherwise due to the original design
Pressure Gauge	Measures the gauge pressure. Chosen as it covers 0-400 kPa which is within the needed range of 50-400 kPa and conforms to 1/4" BSP
Photodiode	Used to detect light which then sends a voltage signal dependant on the intensity of light. Has a moderate sensitivity to red light but has a higher sensitivity for infrared which will be used in further research
DAQ board	Has four channels that can be run simultaneously up to 1MHz
Hot wire	chosen as its range covers the calculated range in Table 3.1
Pressure Regulator	Reduces the pressure to user defined. Chosen as the Proposed range is 50-400 kPa and it covers 0-400kPa
Flowmeter	Rotameter measure volume flow by running air through a tube with a float that is calibrated to certain values. Due to price and time constrictions, It is the closest rotameter calibrated for air, to the proposed flow rates seen in Table 3.1
Red Laser Diode Pointer	Best available laser within time constraints that can be used without training
Hose Air Application Tube	Chosen as it is able to withstand pressures larger than 800 kPa and long enough to reach from the wall to the rig
Solenoid Valve	Valve controlled through electrical pulses. Chosen Due to the ease of use of DC, low power requirements of 12V, max pressure of 1MPa, 1/4" BSP fitting
New Powder Test Section	Designed to fit in with the rig, while ensuring that it is airtight and allows for the laser to pass through the pocket
Red Helium Neon Laser	Brought in for other projects but used due to its higher power, stability of the lasers output and powered from socket, so that there is no voltage drop over time due to battery power loss
Catchment System	Used to catch the powders as they leave the rig. Created to catch the powder without affected the flow from inside the rig
Powders	Supplied from DFE Pharma in coordination with Dr Gerald Hebbink

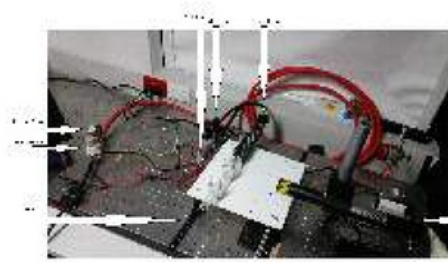
Table 3.5: Parts and the reasonings for the obtainment

pockets from the swivel and using it in conjunction with Figure A.1(b) screw upwards to ensure air tightness until the new testing section was implemented.

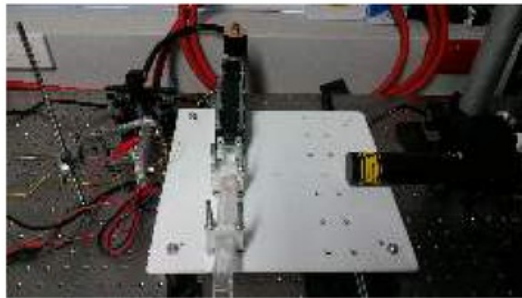
3.3.2 Acquiring and Controlling the Air Flow

This component deals with sourcing the air and then constricting to the properties that is desired. The air was acquired through the use of laboratory air taps that provides compressed air at between 700-800kPa. This is transported from the taps through a hose to the pressure regulator and connected by a hoesetail/Male BSP fitting. This is directly connected to a T intersection by a hex nipple where the gauge is attached allowing for the flow to continue while showing gauge pressure. From the T intersection a long piece of hose is attached to a hoesetail/Male BSP fitting connecting to the flow meter using a hose tail/Male NPT fitting. A long pipe is required here due to a burr in the T intersection creating resonance that needs to be smoothed out before reaching the rig. For the Flowmeter to work correctly it has been clamped to optical posts in an upright position. The flowmeter is then connected to the solenoid valve through hose and hose tail/Male NPT and BSP fittings respectively.

The setup of the solenoid involves attaching it to the DAQ board attachment 9401 and power supply through a transistor. This is because the voltage sent out by the DAQ board is not high enough for the valve to register and open, so it needs to be boosted from a power supply through a transistor. The transistor was mounted on the electrical breadboard and wired as seen in Figure A.5(b) with wires being directly put into the NI9401.



(a) Assembled Rig 1



(b) Assembled Rig 2

Figure 3.3: Assembled Rig

3.3.3 DPI Rig

From the Solenoid valve it enters into the DPI rig. The base plate was attached to optical posts that are connected to rails allowing for motion in one direction seen in Figure 3.3. The DPI rig was bolted together with 2 centimetres above the base plate, with the testing section and tunnel slotting into the grooves and then bolted down with teflon tape around to ensure there are no leaks portrayed in Figure 3.4.

Once this was done air was run through the device at different pressures and flow rates with liquid soap sprayed onto fittings to find if there are any air leaks. (bubbles will appear where there are leaks due to the liquid soap). After Leaks were found, the connections were undone and reapplied with more teflon tape and put back together tightly and checked once again.

Once the leaks were fixed, trial runs with SV004 were used with the addition of a catchment system to the end of the rig. Powders were poured into the pocket and levelled off ensuring a flat initial powder positioning without compression. It should be noted, powders were not compressed into the pocket as this would change the initial variables by creating larger agglomerates and making a greater force to entrain the particles. The pocket was then inserted and pushed up against the testing section to ensure it was completely sealed as seen in Figure 3.5. The solenoid valve was then released for differing



(a) Disassembled DPI Rig 1



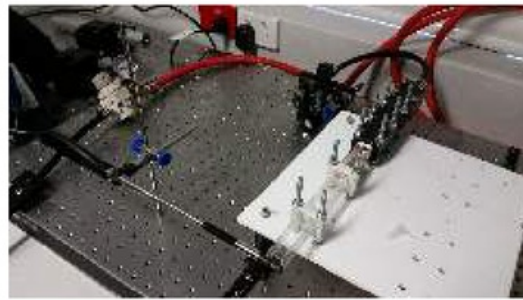
(b) Disassembled DPI Rig 2

Figure 3.4: Disassembled DPI Rig

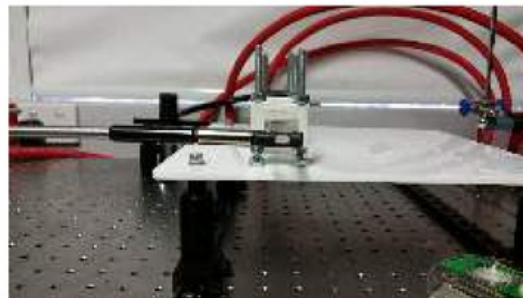


Figure 3.5: Initial Testing Section Assembled

amount of times ensuring entrainment occurred.



(a) Hotwire 1

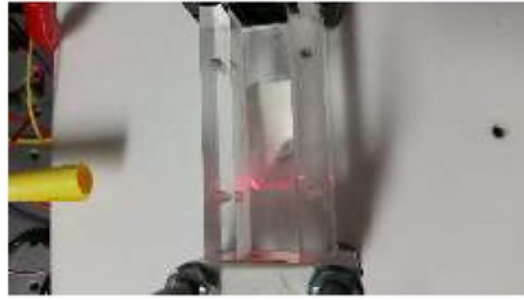


(b) Hotwire 2

Figure 3.6: Assembled Hotwire

3.3.4 Testing Components

For the first component of testing, the hot wire was attached to a three prong clamp to a pole stand that was attached to the optical breadboard with the testing section set in the middle of the tunnel Seen Figure 3.6. Once Testing had been completed it was dismantled and packed away.



(a) Laser Diode Pointer 1



(b) Laser Diode Pointer 2

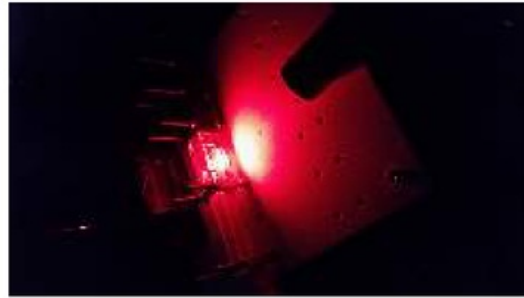
Figure 3.7: Assembled Laser Diode Pointer

The second component is the laser testing. For initial Tests the diode laser pen was used and mounted so that it shined through the testing area as seen in Figure 3.3. The Photodiode was mounted on the electrical breadboard and connected to the DAQ board attachment 9223 through a BNC to crocodile clips wires. The positive wire from the DAQ board is connected to pin 4, while the negative wire is connected to pin 1. (it is possible to boost voltage but was not used for this experiment). The breadboard is then mounted so that the laser light shines upon the photodiode as seen in Figure 3.7. For the Second component the laser pointer is taken out and the HeNe Laser is mounted using its specific supports and shined through the testing section like before. seen in Figure 3.8

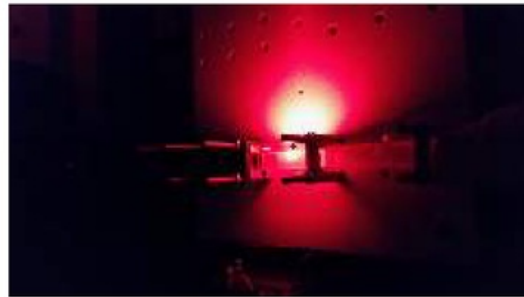
3.3.5 Software Programs and Data Analysis

This component involves the taking of measurements and analysing the data. The hotwire comes with the program meter which when used with the hotwire, tracks the readings from the hotwire and graphs its results in real time. This can then be saved into a csv. file which can be used to interact with programs such as Excel and MATLAB.

To use the photodiode and the Solenoid Valve requires the installation of software from National Instruments to co-ordinate with their devices and software that can be



(a) HeNe Laser 1



(b) HeNe 2

Figure 3.8: Assembled HeNe Laser

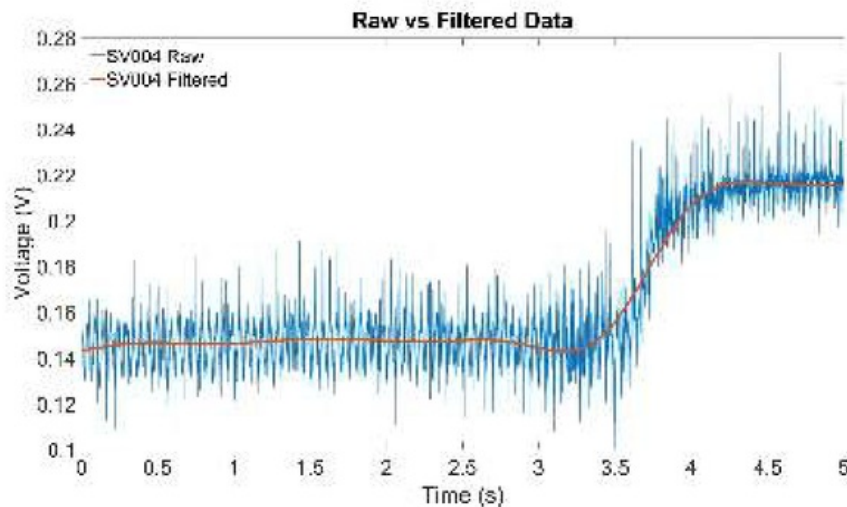


Figure 3.9: Raw Data vs Filtered Data

programmed to control these devices such as labVIEW, which is used in this project. To use labView a Virtual Instrument (VI) is created and programmed to do a set task. The VI for the gathering of data from the photodiode and opening the solenoid valve is seen in Figure A.3. This Vi allows the user to set the range of voltage acquired, determine the sample rate per second, the number of samples and has a trigger setting for the acquisition of data used in the photodiode. It also permits the user to control the solenoid valve by selecting the Frequency of pulses, the duty cycle and the number of pulses it sends.

Once the Data had been acquired it was found to be extremely noisy and was therefore passed through a filter in MatLab to show cleaner and clearer results. The code seen in Figure A.9. This uses the design digital filter function to use a butterworth second-order section filter. It calls a response type that was chosen to be an infinite impulse response lowpass filter, the filter order to be 5, the half power frequency which is a cutoff definition defined by taking halfway from the peak of the maximums at 0.001 using a second order butterworth band filter. This method was used as the filter was found to portray the most refined while still being accurate. This is seen in Figure 3.9.

3.4 Testing

3.4.1 Hot Wire Testing

Through the use of an invasive testing known as a hot wire, the velocities exiting the DPI rig will be found by averaging the results over roughly a 100 samples. Through this we will be able to verify the expected velocities that are coming through from calculations.

To ensure accuracy the hot wire was attached to the optical board through a three prong clamp, bosshead clamp and post.

Initial testing was done using Figure A.1(n) at 100 kPa for a full range of the flowmeters readings between 20-100 l/m in 20 l/m increments. This was done to show the closest correlation to the theoretical calculation seen in Table 3.1 and the expected velocities when the pocket was full of powder.

The next set of testing included the modified testing section taking readings over 100, 200 and 300 kPa readings for a full range of flow meter readings between 20-100 l/m in 20 l/m increments. To find if pressure had any input on the volume readings, and the velocity discovered with actual testing area in place.

The next test involved the complete assembly using the solenoid valve, to see if there was any effect with its implementation over 100, 200 and 300 kPa readings for a 20, 40 and 60 l/m. This was due to the restriction once the solenoid was applied of not exceeding 60 l/m at 100 kPa.

The last hot wire test involved the final setup with the new testing section at 300 kPa for 20, 40, 60 and 80 l/m. The majority of tests used 300 kPa at 80 l/m as it was at these conditions that entrainment readily occurred.

These tests will be used to validate the theoretical results seen in Table 3.1 and to understand the real velocities that occur in the rig.

3.4.2 Laser Setup and Measurements

This involves a non-invasive testing that has been seldom seen for such problems, consisting of a laser and photodiode. The laser will shine through the testing section into a photodiode which sends a voltage to the DAQ board which feeds into LABVIEW to show the results. The basic concept is shown in Figure 3.10

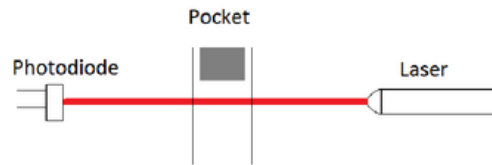
Using the initial remodeled section, control tests were taken with the laser diode pointer first, to examine the quality and consistency of data. This moved into looking into the differences in sample rates and Time, using SV004, at 2mm above the origin, for 2000, 4000 and 10000 Samples/sec for 5 and 10 seconds.

Further tests were done at heights of 5, 7 and 10 mm starting from the origin and moving towards the flow in increments of 2 mm until 12 mm in for 7 seconds. And 5 seconds at 10mm. This is also done for 5mm and 10mm up going away from the flow at 2mm increments up to 8 mm away from the origin for 5 seconds. This is done to portray the areas where data can be obtained.

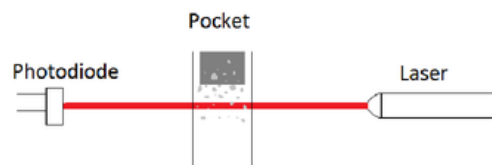
Using the new section allowed for the laser to be shone into the pocket to measure the evacuation times as the pocket was also made of perspex. Using the laser diode pointer at 2.5mm below the origin at 2mm and 12mm towards the flow measurements were taken for 5 seconds using SV004.

The HeNe testing could only be used with supervisor Agisilaos Kourmatzis thus there was a strict time limit in its use. Control tests were taken to examine the quality and consistency of the data and compare with the previous laser diode laser. SV004 was planned to be used in further tests however the powder had become clumpy and was no

longer flowing as it should. Therefore SV 0010 was used at 2.5mm below origin and 15mm towards the flow and repeated four times to ensure consistent results.



(a) Laser Setup 1



(b) Laser Setup 2

Figure 3.10: Basic Diagram of How The Laser is Affected by Particles

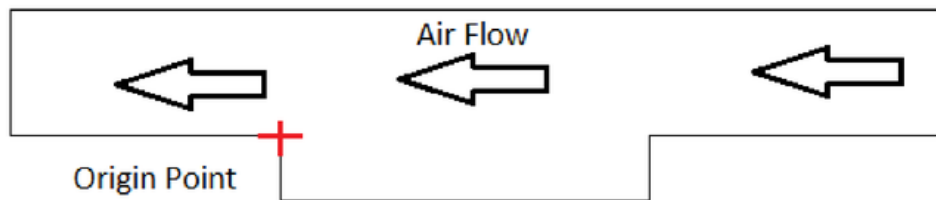


Figure 3.11: Where origin is

Chapter 4

Results

4.1 hotwire

Flow Rate (l/m)	100kPa (m/s)	200kPa (m/s)	300kPa (m/s)
20	2.028	1.908	1.953
40	3.51	3.566	3.589
60	4.992	5.157	5.188
80	6.83	7.186	7.190
100	8.818	9.084	8.835

Table 4.1: Averaged Values for Hotwire Testing With The Pocket Attached

Flow Rate (l/m)	100kPa (m/s)	200kPa (m/s)	300kPa (m/s)	300kPa New Poc
20	2.000	1.983	1.923	1.991
40	4.115	4.18	3.924	3.731
60	7.153	6.571	6.987	6.45
80	N/A	N/A	N/A	12.066

Table 4.2: Averaged Values for Hotwire Testing With Solenoid Attached

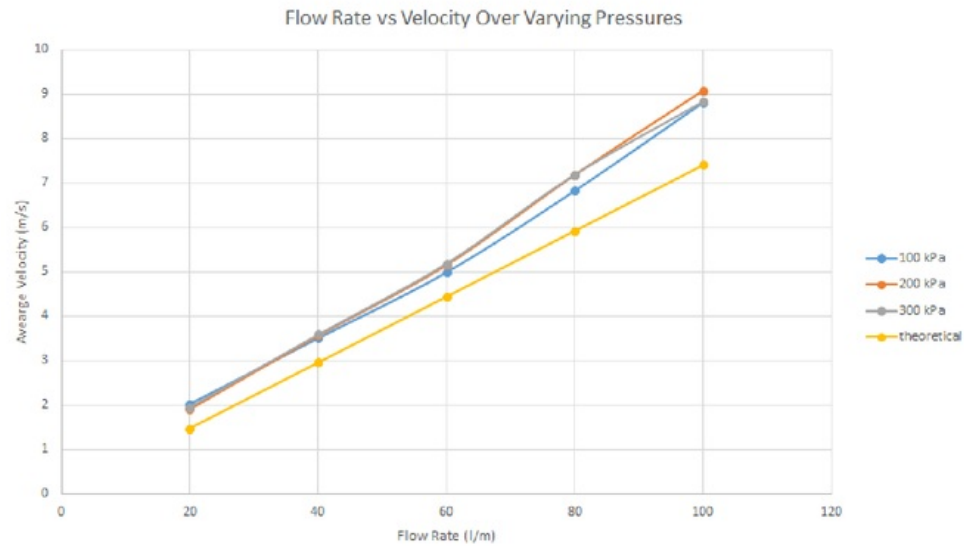


Figure 4.1: Volume Flow Rate vs Velocity of Averaged Values for Varying Pressures from Table 4.1

Flow Rate (l/m)	Single Tunnel (m/s)	With Pocket (test 1) (m/s)	With Pocket (test 2) (m/s)	With Solenoid (m/s)	Theoretical (m/s)
20	1.659	2.028	2.177	2	1.481
40	3.283	3.51	4.06	4.115	2.963
60	4.942	4.992	5.62	7.153	4.444
80	6.237	6.83	7.22	N/A	5.926
100	7.618	8.818	9.002	N/A	7.407

Table 4.3: Averaged Values for Hotwire Testing at 100kPa

Test	Largest ST.DEV
Tunnel	0.1468
With Pocket Test 1	0.1389
With Pocket Test 2	0.0497
Solenoid Test 1	0.0416
Solenoid Test 2	0.0234

Table 4.4: Largest ST.DEV of each Test

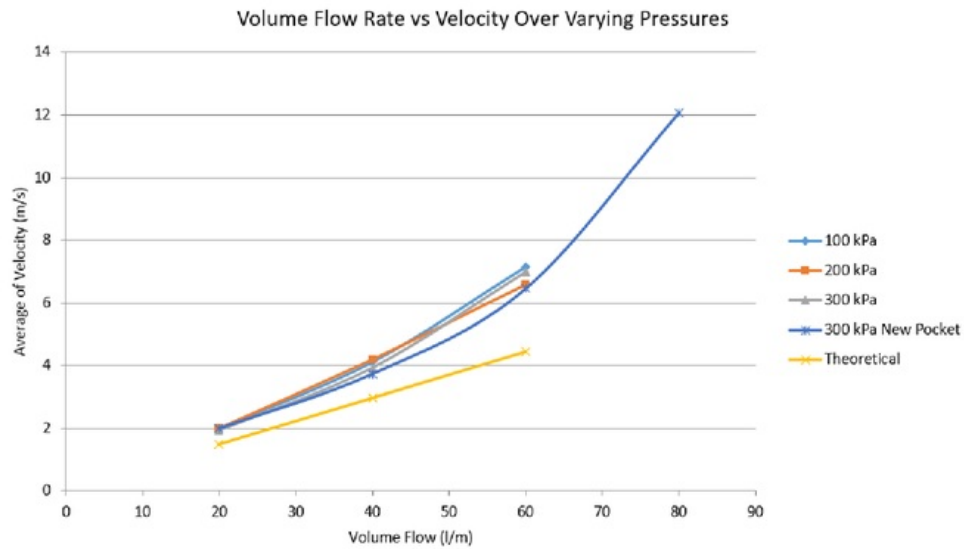


Figure 4.2: Volume Flow Rate vs Velocity of Averaged Values for Varying Pressures from Table 4.2

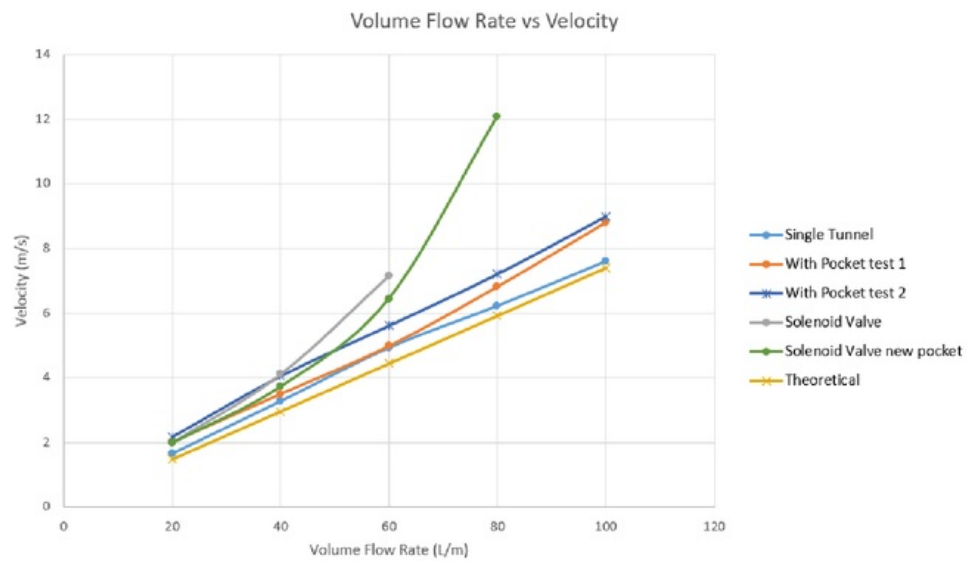


Figure 4.3: Volume Flow Rate vs Velocity of Averaged Values at 100kPa from Table 4.3

4.2 Laser Tests

4.2.1 Control

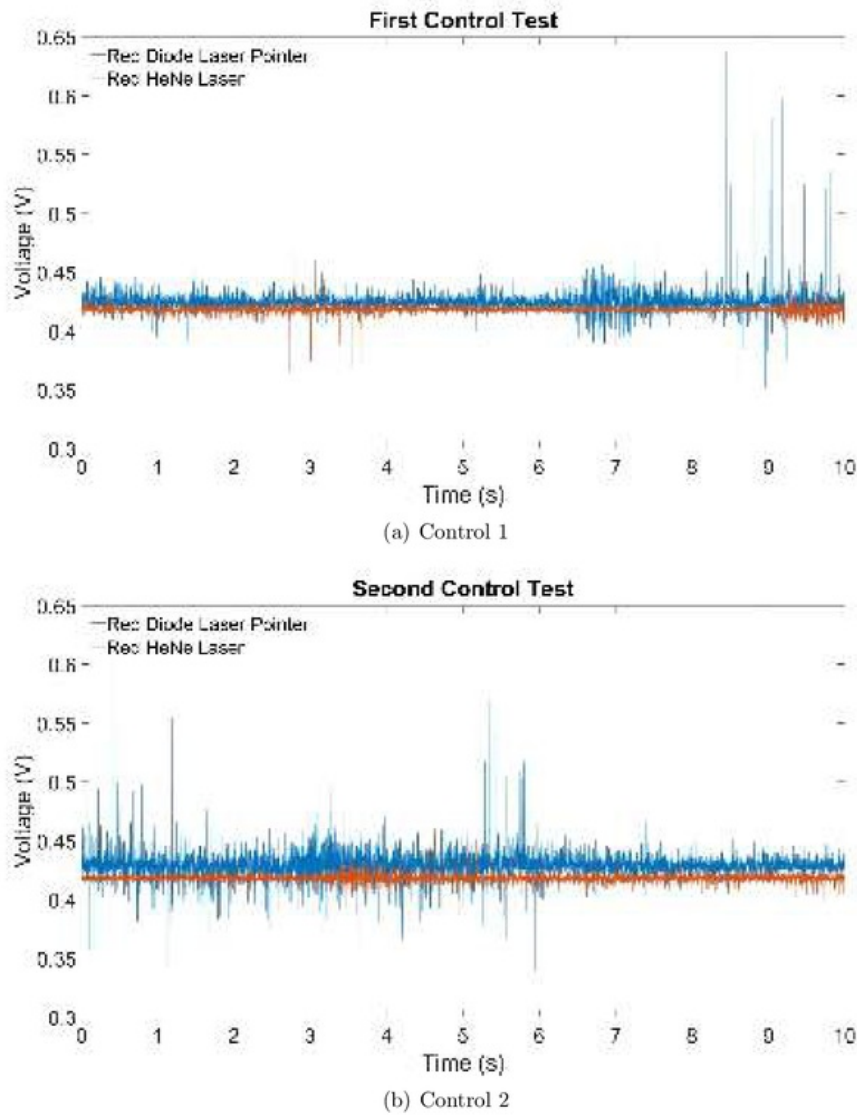


Figure 4.4: control tests between diode and HeNe laser

Control Data shows the data obtained by the photodiode with nothing going on.

4.2.2 Sample Rates and Time Flowing

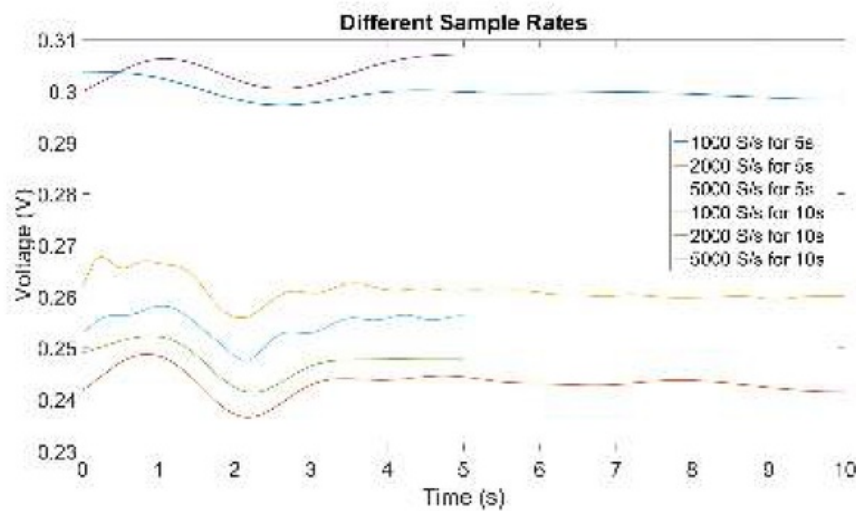
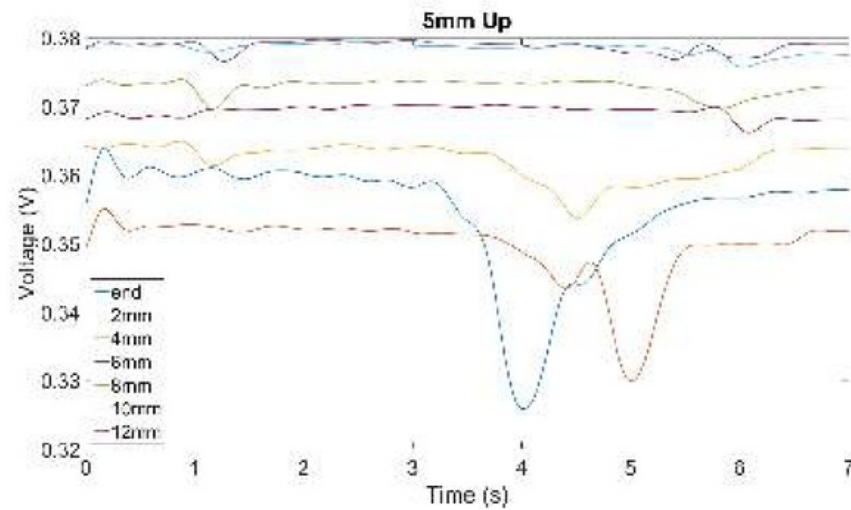


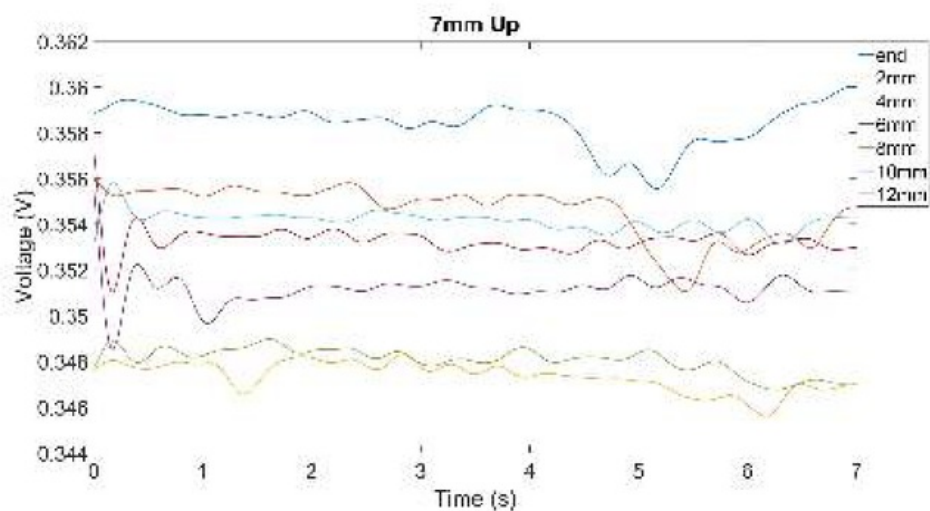
Figure 4.5: Comparison of Different Sample Rates and Time

Notable drops occur for all Sample Rates with the Voltage stabilizing usually by three to four seconds. Original Data and filtered vs Raw Data graphs can be seen in Figure A.10

4.2.3 Locating Detectable Data



(a) 5mm Up



(b) 7mm Up

Data was most strongly found around the origin, raw data and examples of filtered data vs raw data can be seen in Figure ??, Figure ?? and Figure ??

Portrays at Lower heights data is obtainable even as you go further away, raw data and examples of filtered data vs raw data can be seen in ?? and Figure A.15.

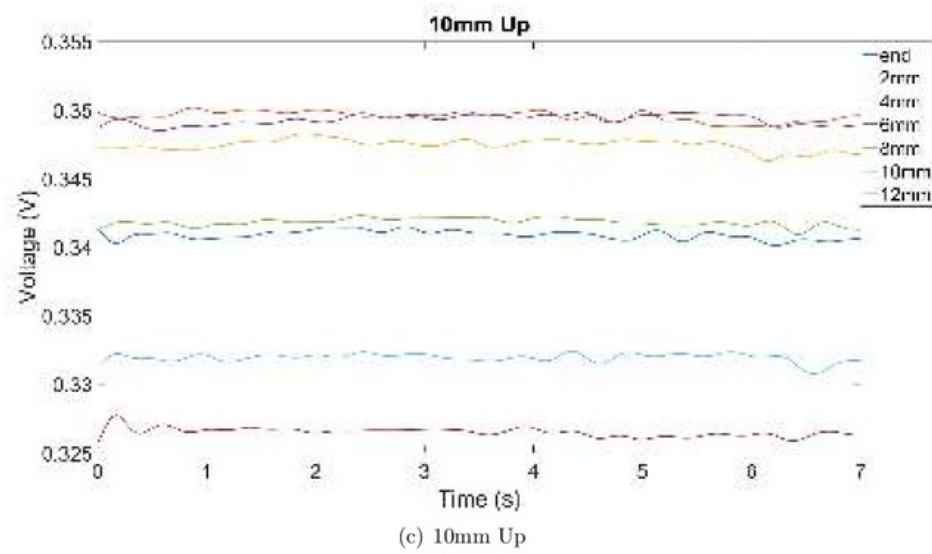


Figure 4.5: Different height going towards flow at 2mm increments

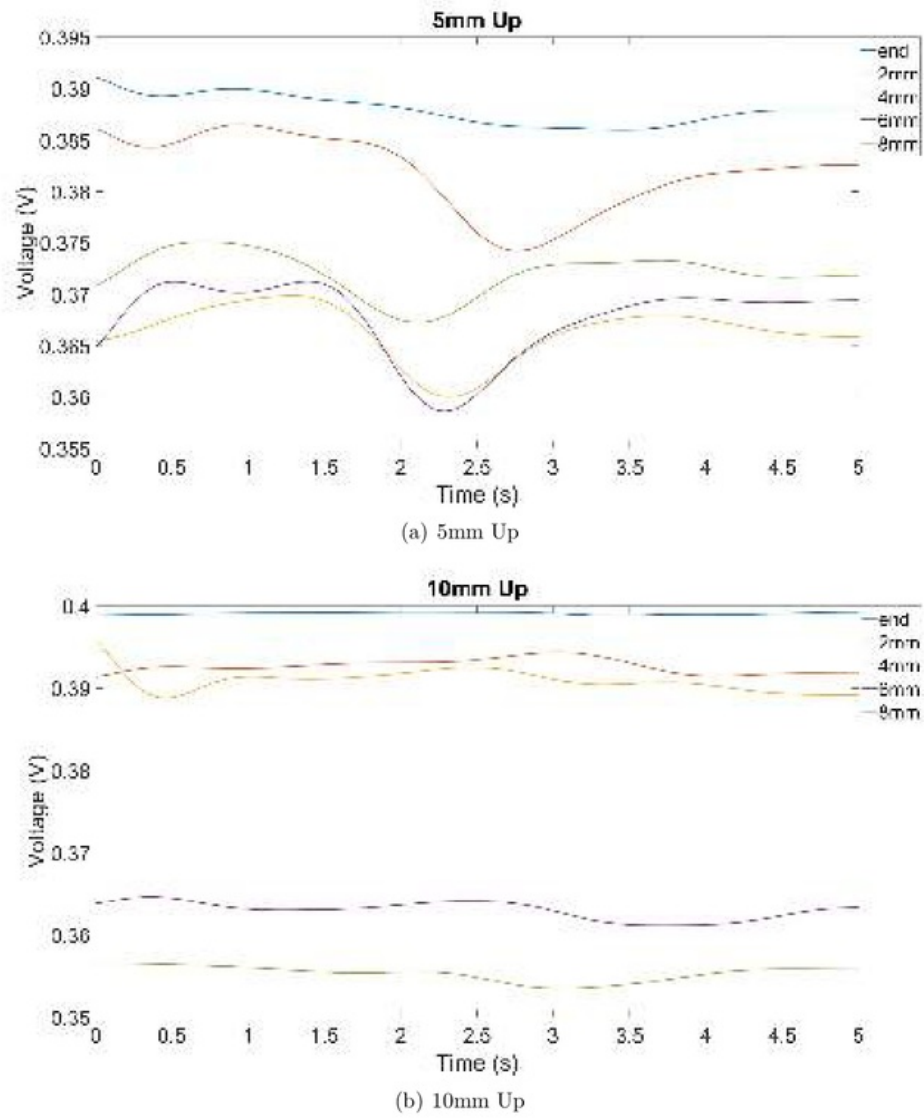


Figure 4.6: Different height going away from the flow at 2mm increments

4.2.4 Laser Directed Through The Pocket

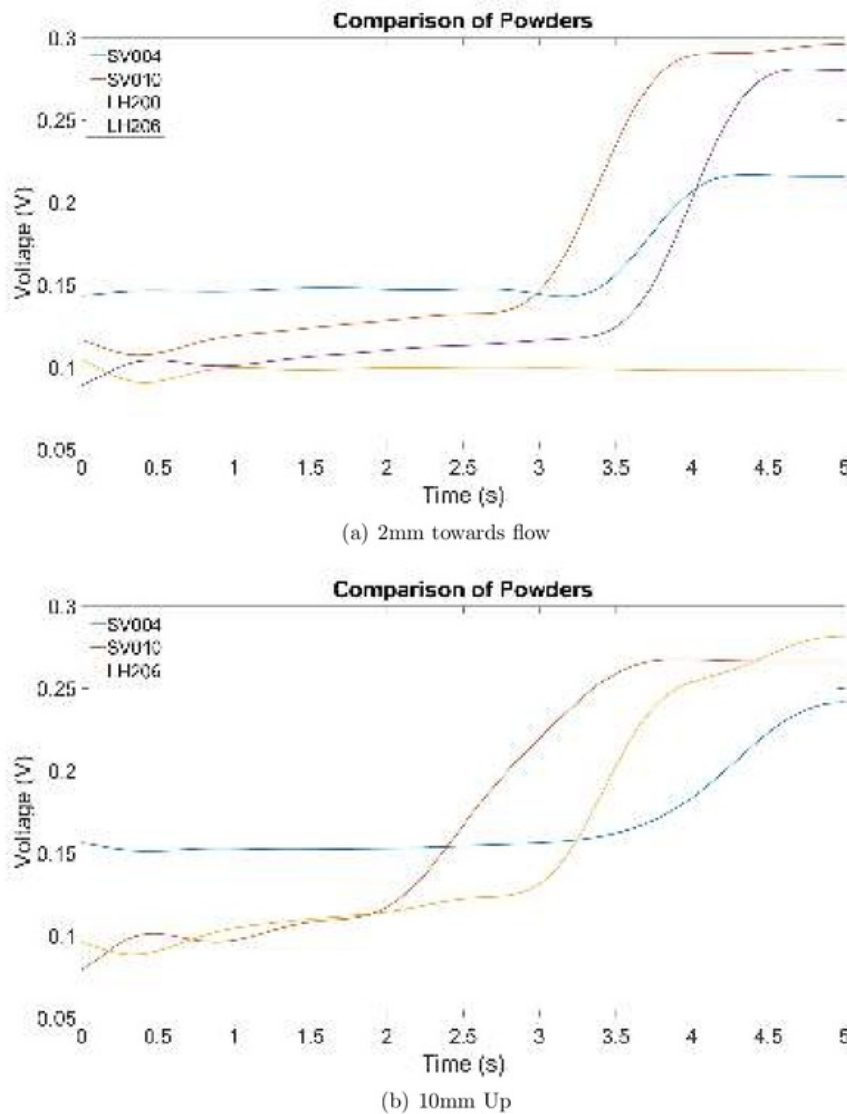


Figure 4.7: Tests at pocket 2mm towards

Portrays evacuation times and provide comparisons between the powders, raw data and examples of filtered data vs raw data can be seen in Figure A.16 and Figure A.17

Powder	Time taken Untill evac- uation from Point (s)	Time With Signficant Change (s)	Voltage Dif- ference of significant change (V)	Gradient of Voltage/Time
SV 004	4.25	3.25-4.25	.015-0.22	0.205
SV 010	3.8	2.8-3.8	0.14-0.29	0.15
LH 200 N/A	N/A	N/A	N/A	N/A
LH 206	4.55	3.4-4.55	0.125-0.28	0.135

Table 4.5: Comparison of powders from Figure 4.7(a)

Powder	Time taken Untill evac- uation from Point (s)	Time With Signficant Change (s)	Voltage Dif- ference of significant change (V)	Gradient of Voltage/Time
SV 004	4.8	3.49-4.8	.0116-0.24	0.095
SV 010	3.75	2-3.75	0.12-0.27	0.086
LH 200 N/A	N/A	N/A	N/A	N/A
LH 206	4.8	2.59-4.8	0.125-0.28	0.07

Table 4.6: Comparison of powders from Figure 4.7(b)

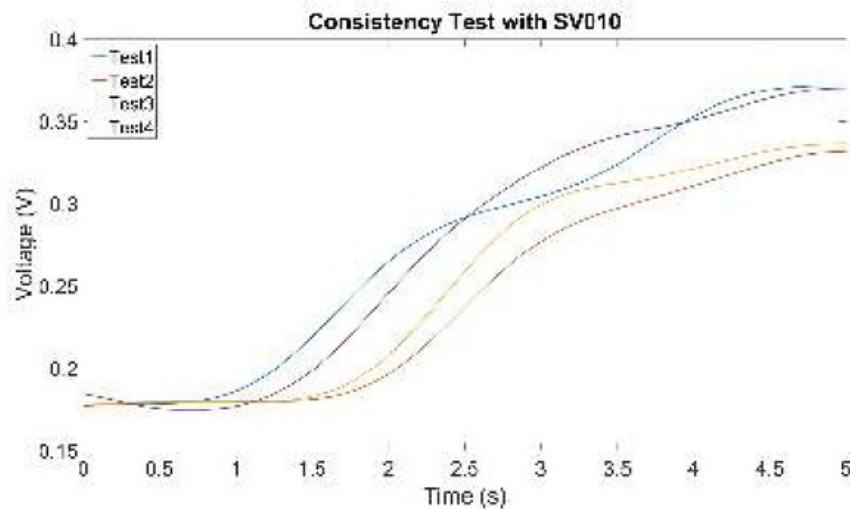


Figure 4.8: SV010 through pocket 2.5mm down adn 15mm towards flow

Shows the consistency of evacuation times for SV010, it has to be noted problems occurred with tests 2 and 3 as the pressure had dropped and entrainment was not as energetic as seen in tests 1 and 4. raw data and examples of filtered data vs raw data can be seen in Figure A.18

Test	Time taken Untill evacuation from Point (s)	Time With Sig- nificant Change (s)	Voltage Differ- ence of sign- ificant change (V)	Gradient of Voltage/Time
Test 1	4.25	0.85-4.25	.018-0.365	0.102
Test 2	4.75	1.75-4.75	0.18-0.325	0.102
Test 3	4.6	1.6-4.6	0.18-0.3	0.04
Test 4	4.6	1-4.6	0.17-0.37	0.056

Table 4.7: Consistency tests using SV010 2.5mm down and 15 mm towards flow from origin

Chapter 5

Discussion

This Project's key aims involve the redesign ,creation, testing of a unique rig and initial findings to provide a basis for further research. This was achieved with varied results but does provide a solid basis to work upon for further projects. This due is to the production of an assembled rig, understanding of positives and negatives of the design and basic results use to develop and understanding of the flow.

5.1 Rig Analysis

This study shows that the assembled rig is able to produce quantifiable data as seen in chapter 4. This means that it will be able to be of use in further research applications in the same format. While quantifiable data was obtained there are improvements that are needed to continue a fully systematic research.

5.1.1 Remodeled Sections

The remodelling of the initial design was able to correct mistakes and support the overall functions of this rig. The major problems occurred through misalignment of the base plate with the optics board, swivel pocket system and the initial testing section.

The misalignment was rectified through the addition of extra holes allowing for the base plate to be bolted onto optical posts that connected to a rail system. This not only created a stable base for the DPI rig but also allowed for a precise measurement of movement in one direction making the testing more accurate and allowing for the laser and photodiode to remain stationary after alignment.

The initial testing section was changed slightly to be able to make an airtight fit, which while working, was not consistently leak free due to incorrect dimensions resulting in a small gap. This was mitigated by having this piece on the opposite side from the incoming flow, thus not affecting the powder bed. Although it did not produce leaks, a small change in the flow would most likely occur as a result of this.

The swivel section that was designed to spin around with four pockets and enter the testing section creating a flush fit and was ultimately scrapped due to the constant

problems that kept occurring. These problems included the swivel not being able to spin due to supports as well as the pocket would only enter the testing section with a sliding motion which was not ideal. This was addressed by separating a pocket from the swivel and using that in tandem with a bolt that was placed underneath that could be used to push up against the pocket to ensure a tight fit.

This was however made redundant when the testing section was changed to the new version. While the new piece created a harder time refilling the powder properly, it was completely airtight and had a clear pocket allowing for evacuation times from areas of the pocket to be able to be acquired. However due to the increased thickness and surface finish, the diffusion of the laser was significant, no longer being a thin beam and thus enlarging the area where light shines upon decreasing the effect of the smaller particles. While the areas where the screws are located do not allow data to be gathered.

5.1.2 Acquiring and Controlling the Air Flow

The acquisition and control of flow worked as expected, with the unexpected finding that the flowmeter was a direct reading which negated the need to calibrate the reading for different pressure. However problems did occur with drops of pressure due too only occasional use. This was easily rectified by checking the pressure gauge before every use. Another source of pressure drop was the occurrence of a burr in the T intersection which was addressed through using a long bit of tube to smooth out the flow again. There is a major problem that will need to be improved in later projects which is the restriction of flow rates due to the addition of the solenoid valve. It was found that for pressures at 100 kPa and 300 kPa it was limited to 60 l/min and 80 l/min respectively. This restriction was due to the size of the valve which was not large enough to allow the volume of air flowing past at such a rate and in turn increases the velocity in an exponential manner due to valve acting as a nozzle and compressing the flow. This can be seen in ???. This can be easily mitigated for future projects through the use of a larger solenoid valve, ensuring that it can comfortably allow flows of up to 100 l/min.

Other than the remodelling of parts that is mentioned before, the DPI rig worked well, with consistent results with no major problems. Despite the success of the rig, due to the pockets size entrainment only occurred at flow rates of above 70 l/min. This in conjunction with the constricted flow due to the solenoid valve meant that testing was done at 300 kPa with a flow rate of 80 l/min so as to ensure decent entrainment. Because of these restrictions and change in velocity gradient, the flow velocity no longer increases linearly and restricts the range of possible tests. Results may have also been slightly skewed due to minor misalignments of the DPI parts in conjunction with the base plate and varying heights of support.

5.1.3 Testing Components

The testing components were able to perform their purpose and deliver quantifiable results thus validating the system's effectiveness. The hotwire produced expected results however

its sampling rate was too low to be able to measure the time it takes to go from 0 to the desired flow rate when the valve is opened. This is an important factor as the time taken to inhale dictates real powder evacuation times. While the laser and photodiode are able to pick up results of particle flow, there were unforeseen problems that occurred. Some amount of diffusion was expected however with the new part there was significant diffusion, such that the beam diffuses out and covers more than the photodiode itself. This creates problems as the range widens, the accuracy for particles that are this small decreases. One other problem that occurred is the level of noise present that continued to spike significantly both in the positive and negative directions and thus not allowing for conclusive evidence of smaller powders passing through. This is most likely due to environmental light coupled with instabilities in the laser as seen in the wild variations of the laser diode in comparison with the HeNe laser in Figure 4.4. Another problem that occurred was the varying voltages in each test, which comes down to having to re-align the laser diode pointer after each stretch of use and the loss of intensity in the laser due to the loss of battery power. These problems however do not occur with the HeNe laser but access was limited to this equipment

5.1.4 Software Programs and Data Analysis

The VIs that were implemented worked extremely well and no problems occurred. Improvements however will need to be made to automatically store, analyse and save data for large amounts of experiments as the exporting process used for this paper was tedious and only suitable for small sets of data. As mentioned before the data was unexpectedly extremely noisy which lead to the need of a filter. The butterworth filter was able to create an accurate following of the data as seen in autoref but for further tests a proper band pass filter should be used.

5.2 Results

5.2.1 Velocity Results

It was found that with the single channel, the velocities correlate very closely being out only by 0.5 m/s. This is due to the assumptions used in the theoretical calculations being closely followed, unlike when the pocket is added with an extra area is added that is not accounted for, with an extra piece attached increasing the chances of changes in the flow. This change may be due to backflow generated by the flow impacting upon the pocket and circulating. This may explain the variation difference seen from the theoretical calculations getting up to 1.3 m/s difference but still following the linear increase with flow.

This shows that although there is some difference that is increasing the velocity it is consistent across the different flow rates. The variation from the solenoid valve however comes due to the constriction of flow that occurs within the valve. The initial velocities follow the trend with the pocket attached however at 60 l/m and above it turns into

an exponential increase as there is a need for higher pressure to increase the flow rate through the small valve area. These results were unexpected as the specs for the solenoid bought had no mention of a maximum flow rate and therefore reduced the range of tests that could occur. Using the theoretical calculations Equation 3.1 the estimated Reynolds number at 300 kPa and 80 l/min is found to be 11878 which is notable turbulent flow.

Errors occur in the velocity due to changes in velocity from turbulence, differ from theoretical due to additions of extra area (the pocket) and the constriction of the solenoid valve.

5.2.2 Laser Results

Control tests that were taken to portray the much more stable intensity of the HeNe laser as it has much less variation as talked about previously. It should be noted that the laser diode pointer has a higher voltage, this could be due to alignment differences and/or the sensitivity differences of wavelength as the laser diode measures between 630-680 nm while the HeNe produces 633 nm. The Test for different sample rates for different times showed that they all roughly had a dip between 1-3 seconds where powders had flown past. However the dips were more pronounced for both the 2000 S/s and 500S/s without much difference. It should be noted noise increased as the sample rate was increased. At this point it can be seen that there was no need to go past 5 seconds as the detectable data has been exceeded.

The next set of tests found that at 5 mm up going towards the flow data was found at the end (origin) between 3.5-5.5 (s), 2 mm in between 4.5-5.5 (s) and a slight drop in 4 mm away between 3.5-6 (s). At 7mm up the end and 2mm with drops over 4.5-6 (s) and 5-6.8 (s) respectively. There are also a significant drop between 0 to 0.5 (s) for 6 and 12 mm in which may be due to environmental influences.

At 5mm going away from the flow, unusually the the end point (origin) does not show any significant drop however 2, 4 6 and 8 mm all show signs of agglomerates passing between 2-3.5 (s), 1.5-3(s) for both 4 and 6, with 1.5-2.5 seconds for 8.

These two tests have shown the general locations where data is available. It has also discovered that the majority of powder pass through these points in roughly a second and that this setup is only able to determine when the majority of particles pass through.

With the new pocket allowing for the laser to be put through the pocket evacuation times were found for 2.5mm into the pocket at 2 and 12 mm. The evacuation times for the area, the time during the evacuation, the voltage and the gradient of voltage over time. Seen in ?? for the sieved powders the smaller SV004 takes between 0.4 -1 second longer as expected as the larger particles are subjected to more lift. Another interesting finding is at 2 mm in it takes roughly 1 second for them all to evacuate while at 12mm they each take between 1.2-1.4 seconds. This may be because the flow is impacting against the end of the pocket and creating a counterflow thus increasing the lift forces exhibited on the particles. Another interesting find is that the gradient at 10 mm in is half that of at 2mm. Which may be due to the before mentioned. Unfortunately LH200 was unable to be tested due to its composition, which was not aerosolising at an increased rate at 80

l/m due to its small size and increased adhesion forces that resist against the shear flow within the 5 seconds of flowing.

The HeNe laser results at 15mm in also show evacuation times to be around 4.25-4.75 seconds however due to the increase in power at 5-10 mW , Light reaches the photodiode before the pocket is actually completely evacuated in this area. This could be a very useful procedure, especially in conjunction with research into finding the voltage readings from a photodiode on varying thickness' of powder, allowing the knowledge of exactly how much powder is leaving at what time. It is also interesting to note that there is always a linear increase of powders being entrained from the data gathered with the laser shining at the pocket.

Errors occur with the laser, photodiode testing due to the diffusion which is mentioned before, the change of alignments of the laser, loss of power in the laser due to batteries dying and enviromental light.

It should also be noted that during the flow shear force no longer becomes the only component once the top layer has been aeorolised with back flow occuring as the powder leaves and air impacts into the pocket.

as the powder leaves increased area for the air to reach changing its reynolds number slightly (seen in velocity readings how single tunnel and with pocket change the velocities)but in combination with the previous point can change the flow significantly.

5.2.3 Consistency

The tests run were found to be extremely consist due to the precise control that the solenoid valve offers and the unchanging nature of the rig. This can be seen in Figure 5.1 which shows both the initial section and the new section powder bed after five seconds. The results found in ?? also show the consistent nature despite test 2 and three having a noticeable pressure drop and thus effect upon the entrainment of the powder.



(a) Pocket after 5 seconds in Initial Pocket



(b) Pocket after 5 seconds in New Pocket

Figure 5.1: Powders left in Pocket after 5 seconds

Chapter 6

Conclusions and Future Work

6.1 Conclusions

This paper has demonstrated the achievement of the the aims of remodelling and assembling a unique rig that is able to perform a systematic study of the effect of reynolds number on different sized particles in simple geometries where the boundary conditions are well defined and the obtainment of early results. This has shown that the rig is able to produce consistent test results and early stage data of the evacuation forces. As a proof of concept it was also able to find problems that occur with this particular design. These include the need for a larger solenoid valve, thinner panes and clearer finishes on the testing section to reduce the diffusion that occurs and the large velocities need to acorlise the the testing pockets size. Despite these problems, there is a bright future for the continuation of this project and projects like this.

6.2 Future Work

This project is expected to be continued upon and further remodeled to produce significant results.

6.2.1 Improvements to Air Flow and Rig

Further work on the airflow involves

- The acquisition of a solenoid valve that will handle flows of up to 100 l/m easily without increasing the velocity due to area restriction.
- Finding the the time it takes for the flow to reach its maximum velocity once the valve has opened as the hotwires sample rate is to slow to respond the sudden increase.
- Finding times taken to exhale amount of varying lung capacity and then correlating that with the rig.

- Future work on the actual DPI rig involves the design and creation of multiple testing sections that narrow i size, allowing for higher velocities and thus higher reynolds numbers while retaining the same volume flow.
- Another improvement is adding the baseplate on y scale so it can move in the x and y directions, allowing for the alignment of the laser and photodiode to not change after alignment and a higher degree of control of placement.
- A major part of the project that was not investigated involves investigating the normal forces involved, using the same flow but in a different section. This will also need new cases to once again narrow the flow and have a clear pocket to find evacuation times.
- The catchment system used for this project was adequate for small amounts of flow, but for further research with longer run times, a better catchment system that will take the flow and redirect it indefinitely is needed.
- One possibility of reducing errors is the inclusion of the tunnel in the testing section instead of separate parts. This will increase parts cost significantly but will stop any chance of leaks or change in flows due to improper connection.

6.2.2 Improvements to Testing Section

There is a noticeable amount of improvement that can be done to ensure more accurate and indepth testing.

- This includes the use of two lasers being used one after the other with little space in between allowing to compare the data of particles going past both lasers, thus being able to find the velocity of the particles travelling through. This would involve mirrors that redirect the beam to photodiodes as ideally the lasers would be to close for separate photodiodes to get accurate independant results.
- The addition of beam splitters before the laser goes into the testing section, would allow for the correlation between an uninterrupted laser and the other going through the test section. By doing this any variations can be compared to detect if it was a fluctuation from the laser or the particles interrupting the beam.
- By soldering wires onto the photodiode, it would expand the movement of its placement, allowing it be closer to the testing section.
- If the noise is determined to be due to inteference of the wires, aluminium wrapping can be used to shield them, to ensure an untampered signal.
- Black material beneath the laser ligth and a black cloth covering the rig would allow for cleaner readings, completely blocking out natural light and the reflective surface of the base plate and optical board.

- The use of the Firefly PIV imaging laser in conjunction with the high speed camera can be used to visualize the flow, determine particle seizures and spray patterns.

6.2.3 Improvements to Analysis and Software

- Repitiveness of tests to ensure accurate data
- Advancing Labview VI to take data and correlate it in MatLab automatically




Chapter 7

Abbreviations

MDI	Metered-Dose Inhalers
DPI	Dry Powder Inhalers
FPF	Fine Particle Fractions
CFD	Computational Fluid Dynamics
COPD	Chronic Obstructive Pulmonary Disease
DEM	Discrete Element Method
API	Active Pharmaceutical Ingredients
SABA	Short Acting Beta Agonist
SAMA	Short Acting Muscarinic Agonist
LABA	Long Acting Beta Agonist
LAMA	Long Acting Muscarinic Agonist
ICS	Inhaled Corticosteroids
VI	Virtual Instrument

Appendix A

Figures



General Risk Assessment Sheet

General Information - Reason for this Risk Assessment: <input checked="" type="checkbox"/> New task <input type="checkbox"/> New Information <input type="checkbox"/> Change to existing work task/object/tool			
What is being assessed - Description of Task/Activity: Compressed air from the lab taps will be flowed through a pipe into a setup involving a pressure regulator, pressure gauge, flowmeter, solenoid valve and medical air pipes. The use of laser pointing through Pargos into a photodiode.			
Where is the activity/task undertaken: Location/Building: B14 Date of Assessment: Audit/Visit: Highways Floor/Number: 0 Institute/Office: Department/unit: Mechanical			
Who undertook the assessment - Assessed by: Checked by: Ready To:			
Task - Workplace conditions: Comments:			
List the systems of work for the Activity/Task - • Training Procedures • Equipment • PPE			
Are there resources that you will use in undertaking the assessment? • Knowledge/skills • Equipment • Available • Code of Practice • PPE • Training • Task only skills • Unaided/limited vision • Equipment			

(a) Risk Assessment 1

Identify the Hazards associated with the task / activity.

For each of the following prompts:

- Check the box for each hazard that may potentially exist for the activity/task
- Determine and record a risk rating (see the Risk Matrix)
- In the comments box, describe when and where the hazard is present
- Specify the risk control to perform the Hierarchy of Control at right, for each assessed or proposed risk control
- Provide a control description for each assessed or proposed risk control

Hierarchy of Control (Control Type)

E - Elimination
 R - Substitution
 En - Engineering
 P - PPE
 C - Control
 A - Administrative (Training, Inspection)
 P - PPE

Activity/Task Hazard Identification	Risk Rating	Comments (e.g., where and when the hazard is present)	Control Type	Control Description	
				Current	Proposed
Is there potential for? <input type="checkbox"/> Being cut or stabbed <input checked="" type="checkbox"/> Slips, trips and/or overexertion <input type="checkbox"/> Electric shock <input type="checkbox"/> Manual handling, Repetitive <input type="checkbox"/> Infection agents or chemicals <input type="checkbox"/> Vibration <input checked="" type="checkbox"/> Other hazard (specify): Blinded	Low Very Low Medium	Blow Change not properly changed, disconnecting hose while there is still air pressure Small laser is pointed directly at eye for adjustment period of time H2SO4 laser hits eye	A A C, A, PPE	Hoses connected into a ring with buildup of Pressure Use of low pressure laser Use of high Pressure laser	Before any change air is turned off and pressure released Use with Care, always have pointed below eye level In both guarding system, wearing goggles that filter out the laser's spectrum of light, Only use with experience

(b) Risk Assessment 2

Workplace Conditions Hazard Identification	Risk Rating	Comments e.g. where and when is the hazard present	Control Type	Control Description	
				Current	Proposed
Is there potential for? <input type="checkbox"/> Extremes of temperature <input type="checkbox"/> High wind or humidity <input type="checkbox"/> Inadequate light <input type="checkbox"/> Dusts, fumes or vapours <input type="checkbox"/> Exposure to UV or other radiation <input checked="" type="checkbox"/> Emergency situations <input type="checkbox"/> Other factors – (specify) _____	Very Low	Emergency Situation occurs in the Lab such as a fire or chemical	A/		Knowledge of Safety Protocols

Notes:

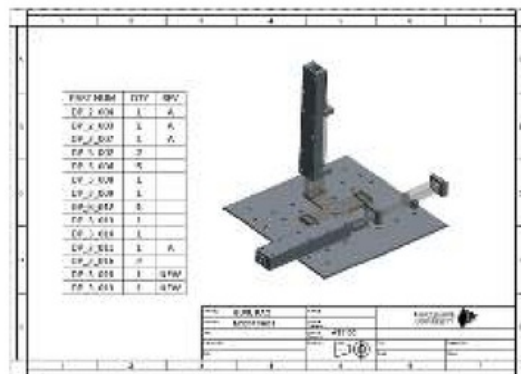
HeNe laser is only to be used with Supervisor Agi Kourmatzis

(c) Risk Assessment 3

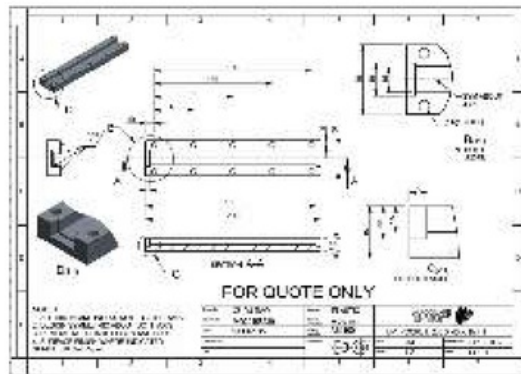
IMPLEMENTATION OR ESCALATION PLAN			
<ul style="list-style-type: none"> Determine the person responsible for deciding upon and implementing the proposed controls. Obtain the authorisation of the Management Representative. Ensure the HSR (if applicable) has been consulted. Ensure the person(s) performing the Activity/Task have been consulted. 			
Person Responsible or Escalated to		Controls Due Date	
Signature of Management Representative	Agisilios Kourmatzis	Due Date	30/8/2016
Signature of Health and Safety Representative		Due Date	
Signature of person performing task/activity	Bradley Yip	Due Date	30/8/2016

(d) Risk Assessment 4

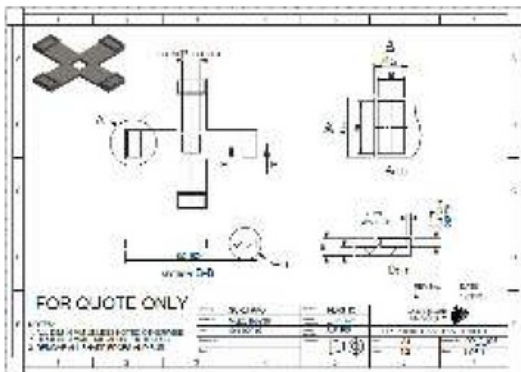
Figure A.0: Risk Assessment of Project



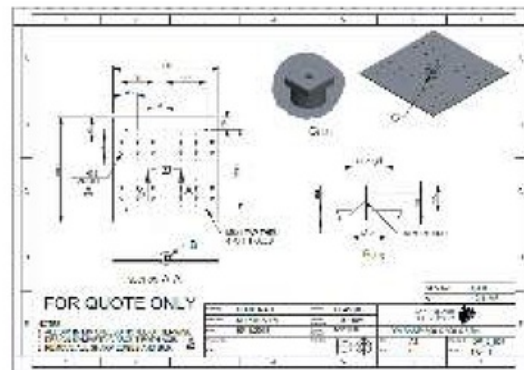
(e) DPI Assembled



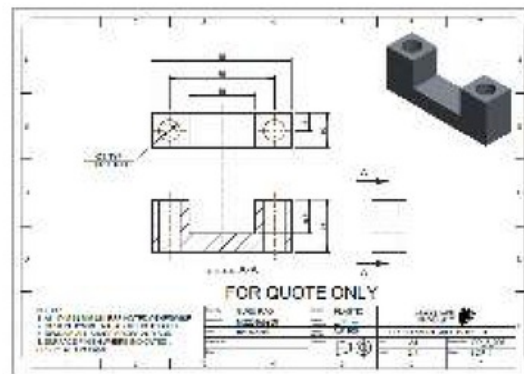
(f) DPI Pt 1

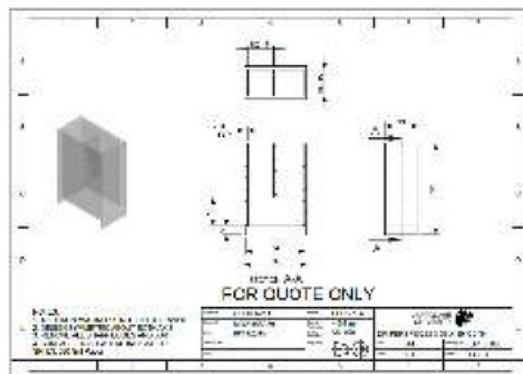


(g) DPI Pt 2

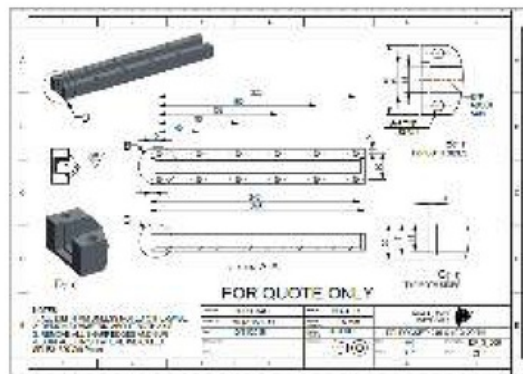


(h) DPI Pt 3

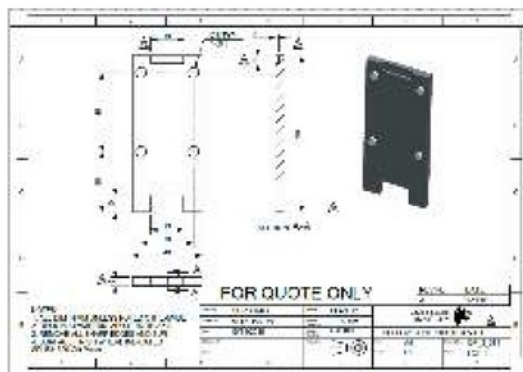




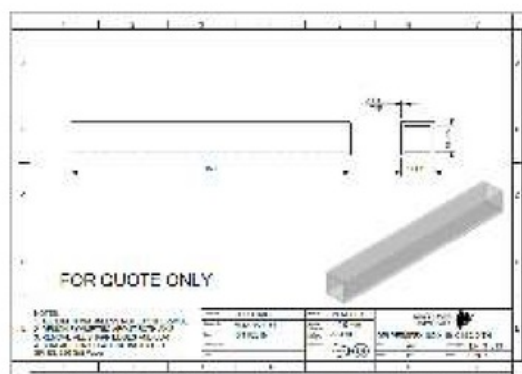
(k) DPI Pt 6



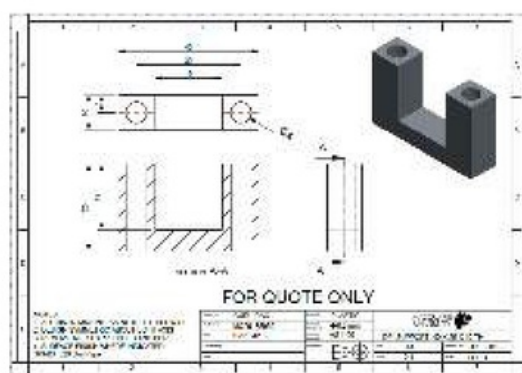
(l) DPI Pt 7



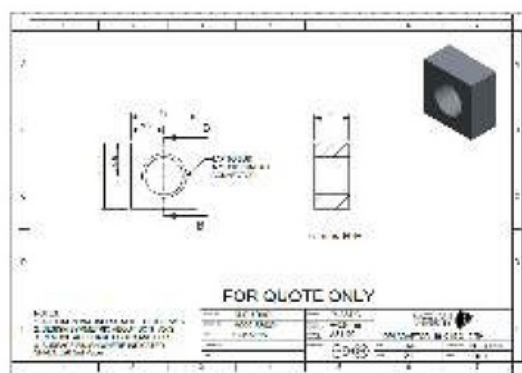
(m) DPI Pt 8



(n) DPI Pt 9

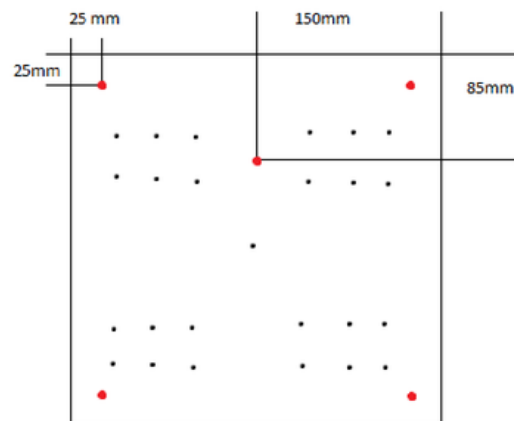


(o) DPI Pt 10

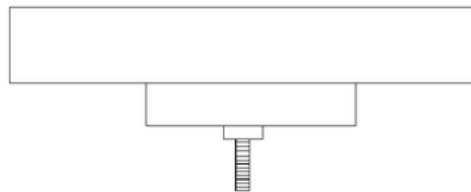


(p) DPI Pt 11

Figure A.0: Engineering Sketches of the Dry Powder Inhaler Rig



(a) Schematic of The New 8mm Holes Drilled Into The Base Plate, New Holes in Red, The Four Outside Holes are Symmetrical

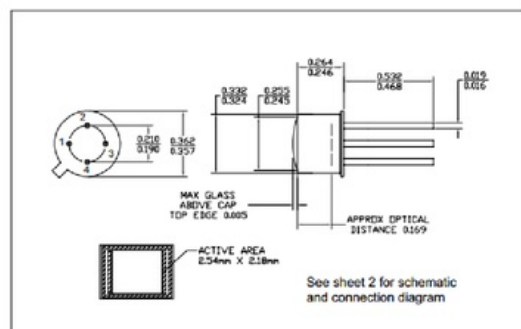


(b) Side View of Bolt Supporting the Pocket

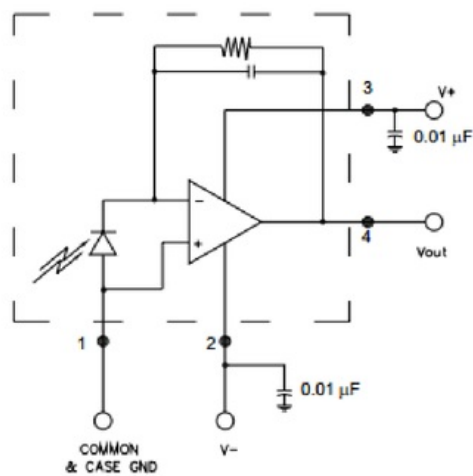
Figure A.1: Overview of Remodeled Parts



(a) Photodiode Specification



(b) Photodiode Schematic



Note: Components shown outside the dashed area are external to the device, and must be supplied by the user.

(c) Photodiode Circuit

Figure A.2: Photodiode Specifications [4]

General Specifications

Display	46.7mm×60 mm larger LCD display
measurement	Dual function meter's display.
	m/s (meters per second)
	km/h (kilometers per hour)
	ft/min (feet per minute)
	MPH (miles per hour)
	knots (nautical miles per hour)
	Temp. — °C, °F
	Data hold.
Memory	Maximum and Minimum with recall
Sampling	Approx. 6.8 sec.
Operating Temperature	0°C to 50°C (32°F to 122°F)
Operating Humidity	Less than 80% RH
Power Supply	9V battery
Power Current	Approx. DC 60–90mA
weight	280g
Dimension	210mm×75mm×50mm
Accessories included	Hot wire sensor 9V battery

Electrical Specifications

Air Velocity			
Measurement	Range	Resolution	Accuracy
m/s	0.1–25.0m/s	0.01m/s	±(5%+1d)reading Or ±(1%+1d)full scale
km/h	0.3–90.0km/h	0.1km/h	
ft/min	20–4925/min	1ft/min	
MPH	0.2–55.8 MPH	0.1MPH	
knots	0.2–40.5knots	0.1knots	
Notes:			
m/s-meters per second	km/h-kilometers per hour		
ft/min-feet per minute	MPH miles per hour		
knots-nautical miles per hour			
Temperature			
Measuring Range	0°C to 50°C (32°F to 122°F)		
Resolution	0.1°C/0.1°F		
Accuracy	±1°C/±.8°F		

Figure A.4: Hot Wire Anemometer Specifications [5]

FEATURES:
 * High Power Dissipation
 $P_D = 150 \text{ W}$ ($T_C = 25^\circ\text{C}$)
 * High DC Current Gain and Low Saturation Voltage
 $hFE = 15-80 @ I_C = 5 \text{ A}, V_{CE} = 4 \text{ V}$
 $V_{CE(sat)} = 1.4 \text{ V (Max.)} @ I_C = 5 \text{ A}, I_B = 0.8 \text{ A}$

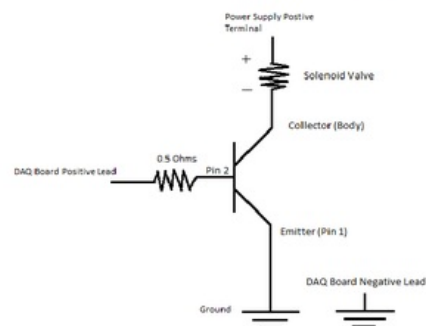
MAXIMUM RATINGS

Characteristic	Symbol	Rating	Unit
Collector-Emitter Voltage	$V_{CE(sat)}$	140	V
Collector-Emitter Voltage	V_{CE}	160	V
Collector-Base Voltage	V_{CBO}	160	V
Emitter-Base Voltage	V_{EB0}	7	V
Collector Current-Continuous Peak (1)	I_C $I_{C(sat)}$	15 30	A
Base Current-Continuous Peak (1)	I_B $I_{B(sat)}$	4.0 15	A
Total Power Dissipation @ $T_C = 25^\circ\text{C}$ Derate above 25°C	P_D	150 0.957	W W/ $^\circ\text{C}$
Operating and Storage Junction Temperature Range	T_J, T_{stg}	-65 to $+200$	$^\circ\text{C}$

THERMAL CHARACTERISTICS

Characteristic	Symbol	Max	Unit
Thermal Resistance Junction to Case	$R_{\theta JA}$	1.17	$^\circ\text{C/W}$

(a) Transistor Schematic [46]



(b) Transistor Circuit

Figure A.5: Transistor Specifications

[illegible]

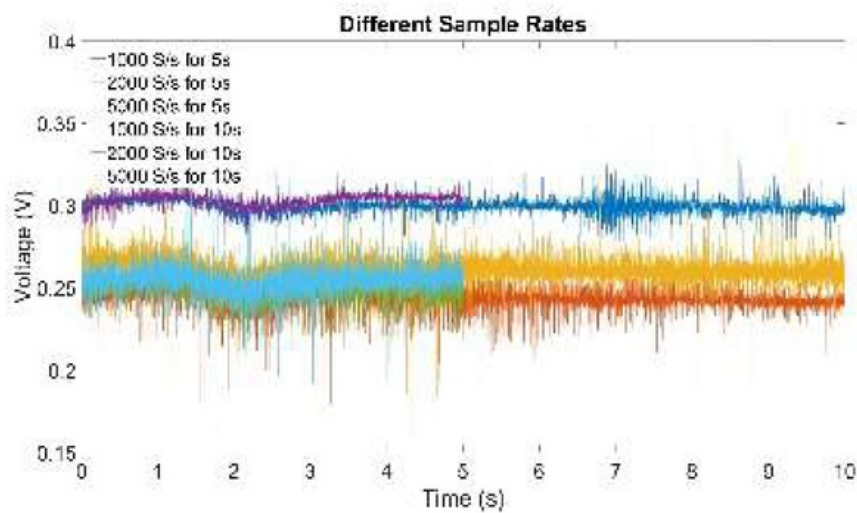
Brand	SMC
Catalogue Page Number	12-33
Maximum Flow L/min @ 6 bar	455
Minimum Order Quantity	1
Order Quantity Multiple	1
Port Size BSP inch	1/4
Port Size BSP mm	6
Standard Pack Quantity	1
Thread Type	BSP

Media Monitored	Gas
Device Type	Flow Indicator
Minimum Flow Rate	10 L/min
Maximum Flow Rate	100 L/min
Pipe Diameter Range	1/8 in
Connection Type	1/8 NPT Female
Maximum Pressure	6.9bar
Material	Polycarbonate
Maximum Media Temperature	+65°C
Maximum Operating Temperature	+65°C

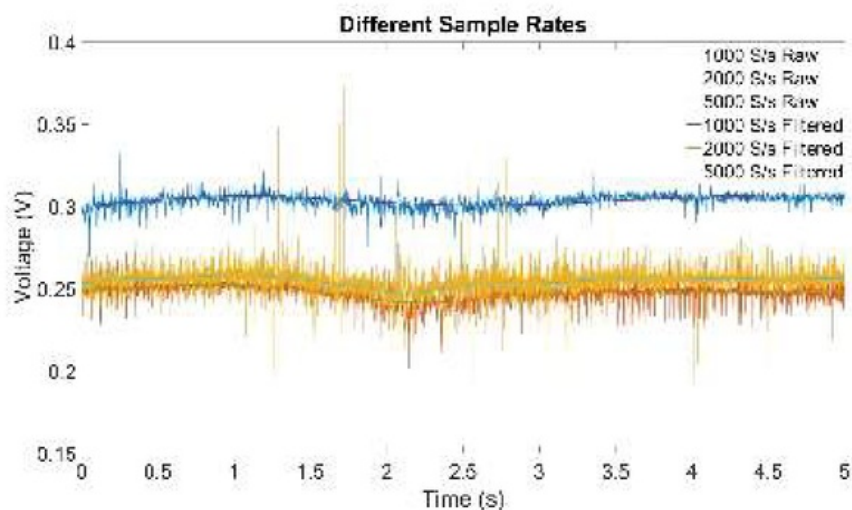
```

d = design('1t1' 'lowpassfilt', 'FilterOrder', 5, 'HalfPowerFrequency', 0.001, 'DesignMethod', 'butter');
y = fitfilt(d, test1);
y2 = fitfilt(d1, test2);
y3 = fitfilt(d1, test3);
y4 = fitfilt(d1, test4);
z = plot('T,y,T,y2,T,y3,T,y4');
legend('test1','test2','test3','test4');
title('Consistency Test with SV010');
xlabel('Time (s)');
ylabel('Vol%age (V)');

```

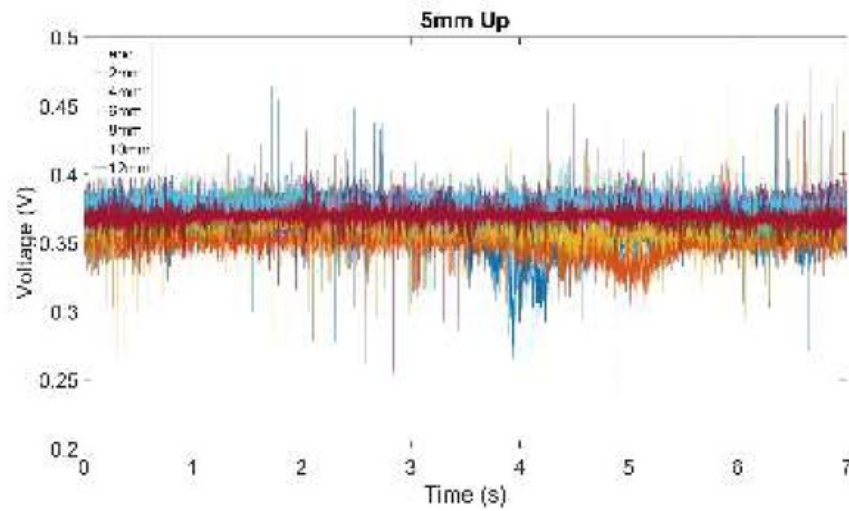


(a) Raw Data For Different Sample Rates and Flow Times

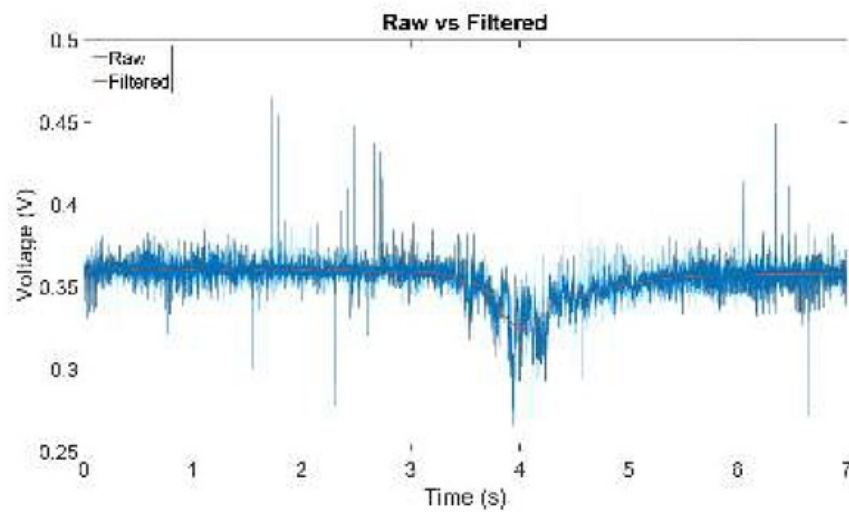


(b) Raw Vs Filtered Data For Different Sample Rates and Flow Times

Figure A.10: Raw and Raw Vs Filtered Data

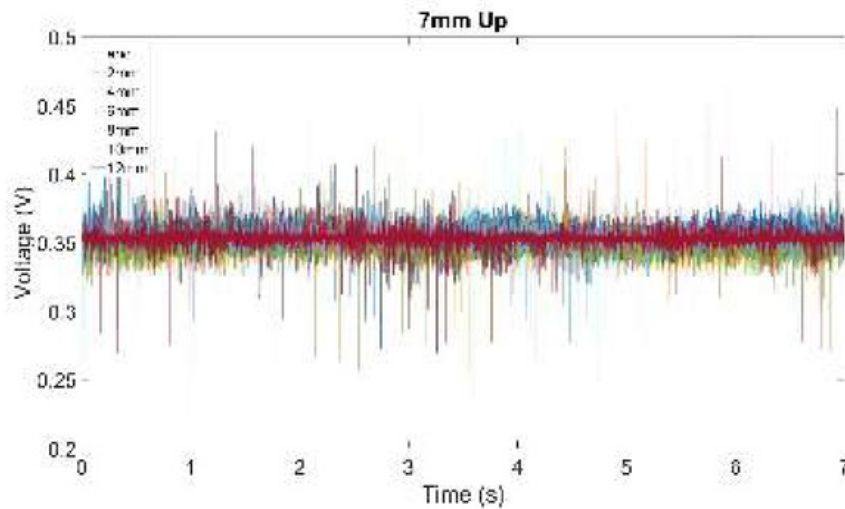


(a) Raw Data For 5mm Up Moving Towards The Flow

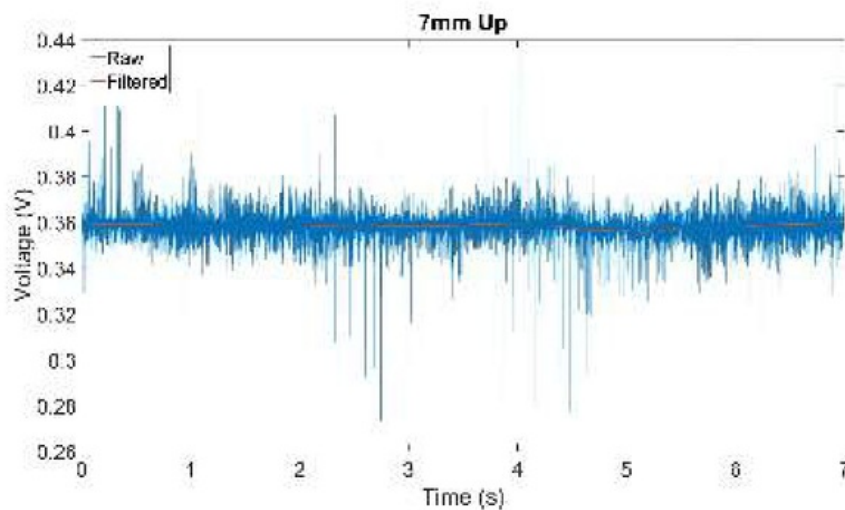


(b) Raw Vs Filtered Data For 5mm Up Moving Towards The Flow

Figure A.11: Raw and Raw Vs Filtered Data

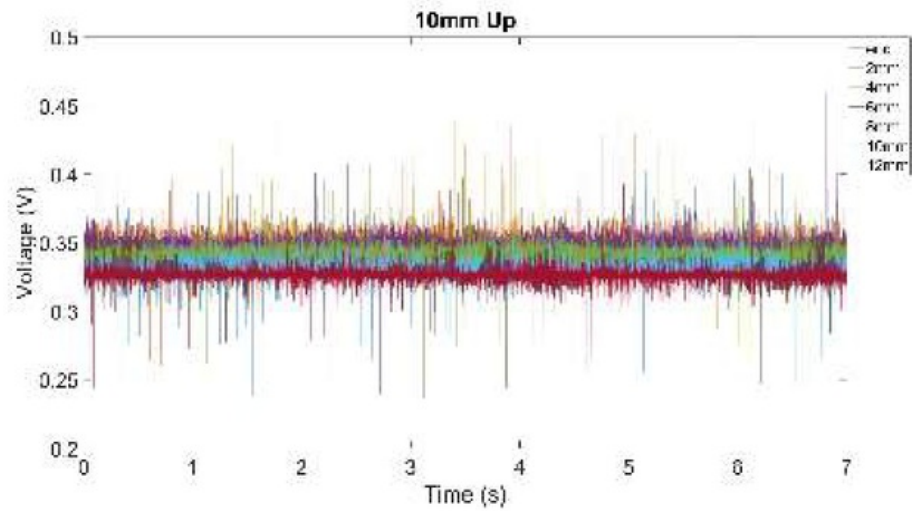


(a) Raw Data For 7mm Up Moving Towards The Flow

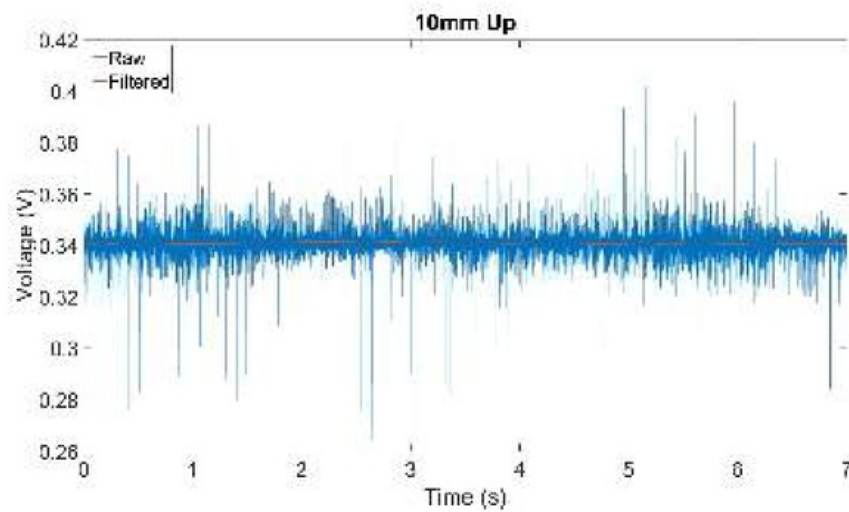


(b) Raw Vs Filtered Data For 7mm Up Moving Towards The Flow

Figure A.12: Raw and Raw Vs Filtered Data

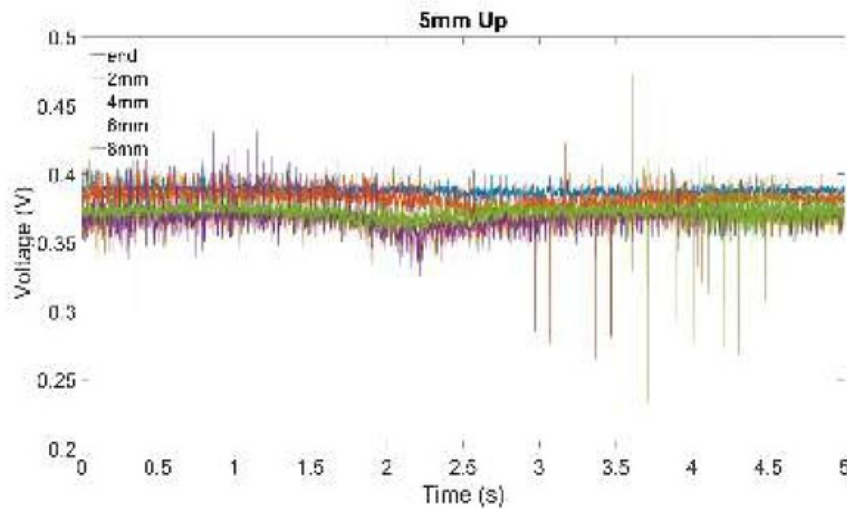


(a) Raw Data For 10mm Up Moving Towards The Flow

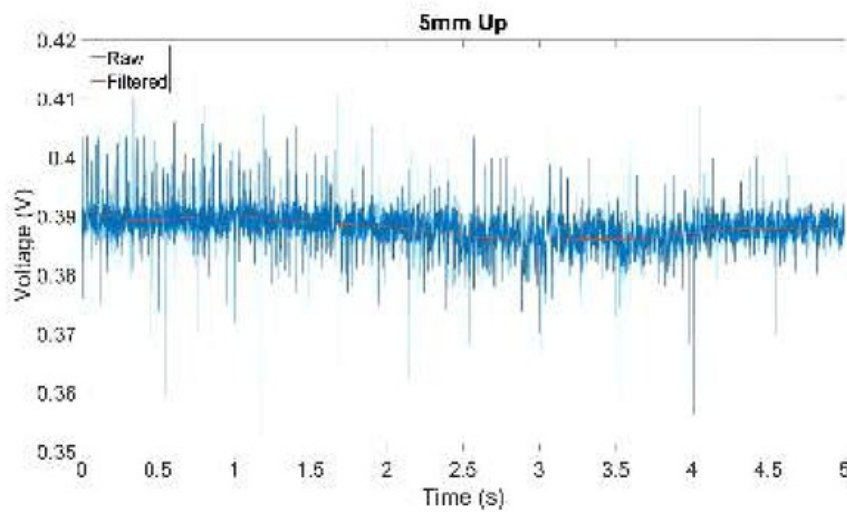


(b) Raw Vs Filtered Data For 10mm Up Moving Towards The Flow

Figure A.13: Raw and Raw Vs Filtered Data

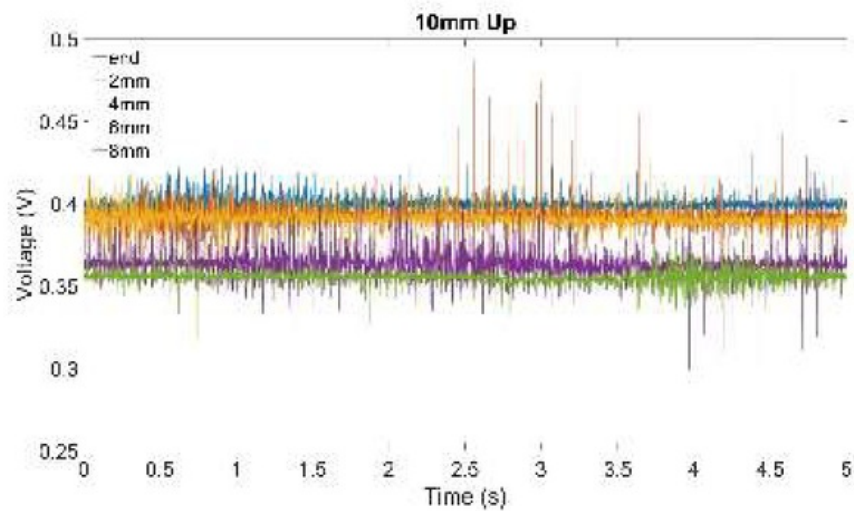


(a) Raw Data For 5mm Up Moving Away From The Flow

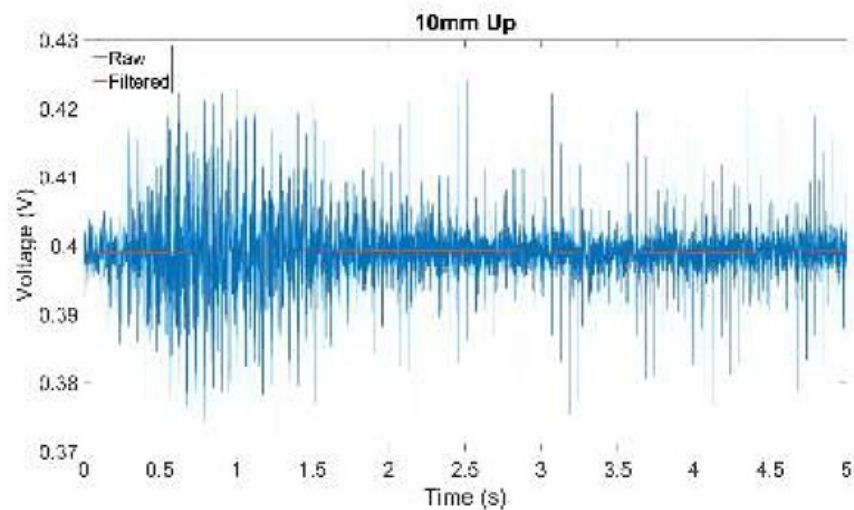


(b) Raw Vs Filtered Data For 5mm Up Moving Away From The Flow

Figure A.14: Raw and Raw Vs Filtered Data

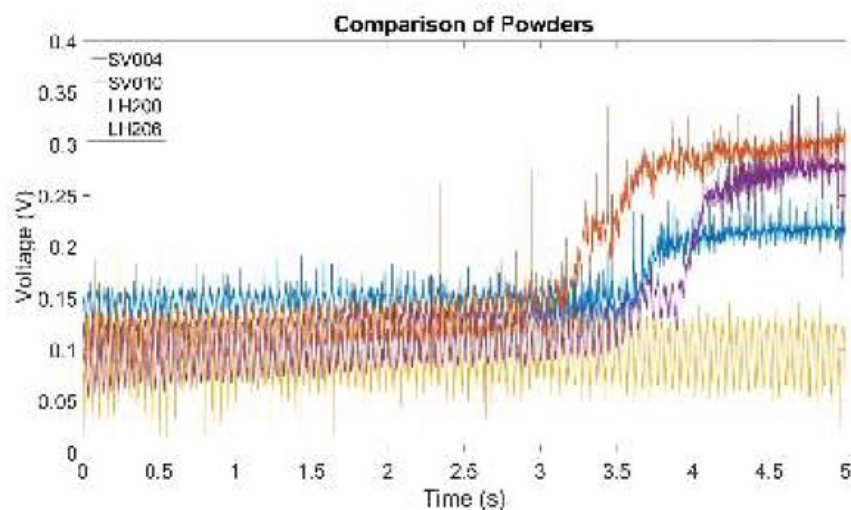


(a) Raw Data For 10mm Up Moving Away From The Flow

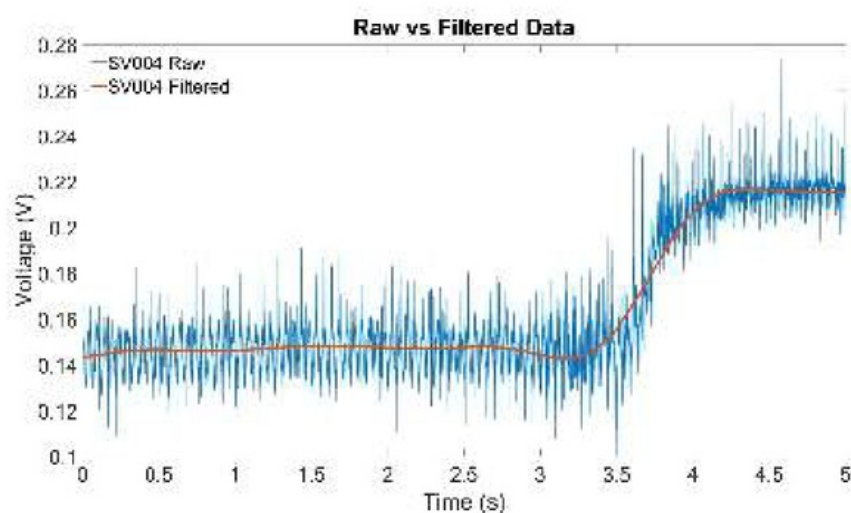


(b) Raw Vs Filtered Data For 10mm Up Moving Away From The Flow

Figure A.15: Raw and Raw Vs Filtered Data

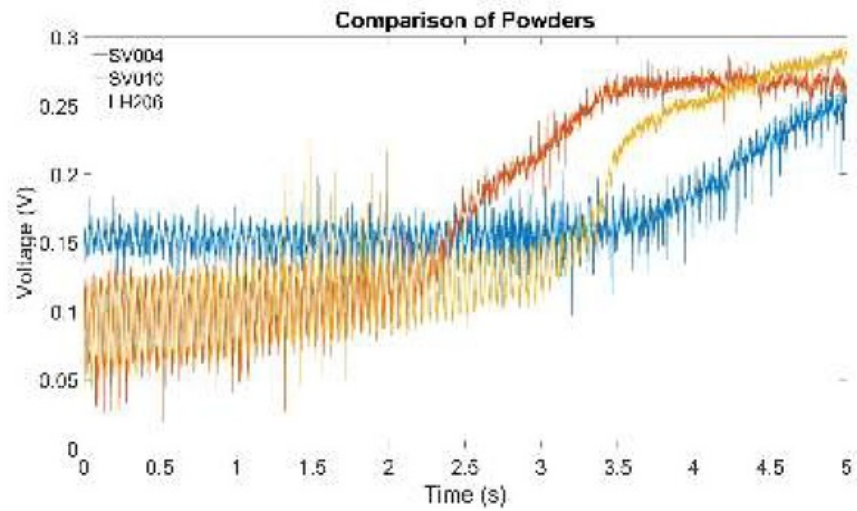


(a) Raw Data For Comparison of Powders 2mm into Pocket

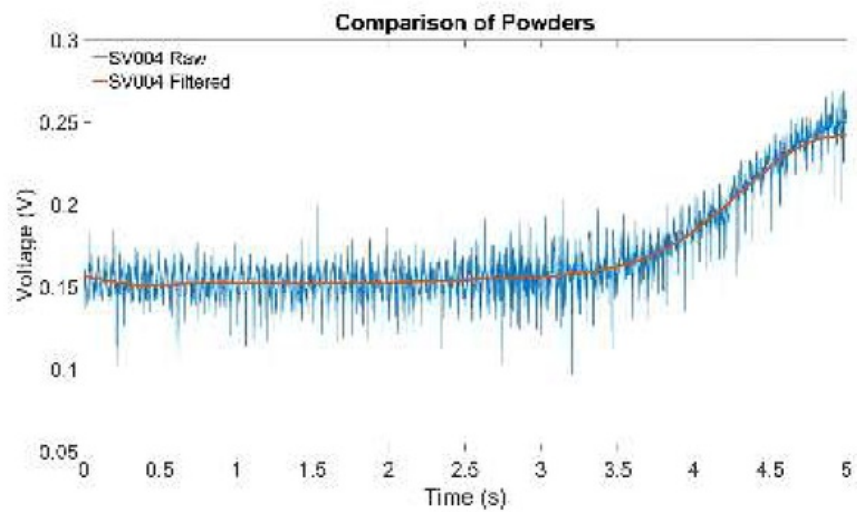


(b) Raw Vs Filtered Data For Comparison of Powders 2mm into Pocket

Figure A.16: Raw and Raw Vs Filtered Data

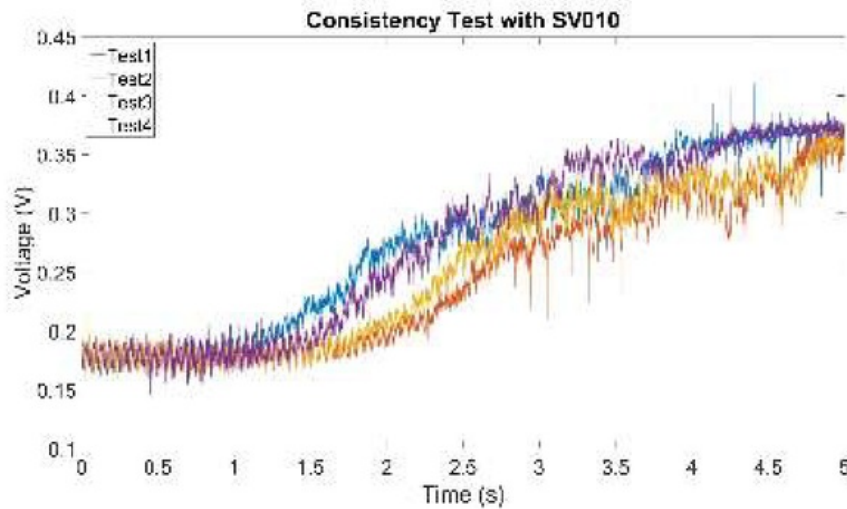


(a) Raw Data For Comparison of Powders 10mm into Pocket

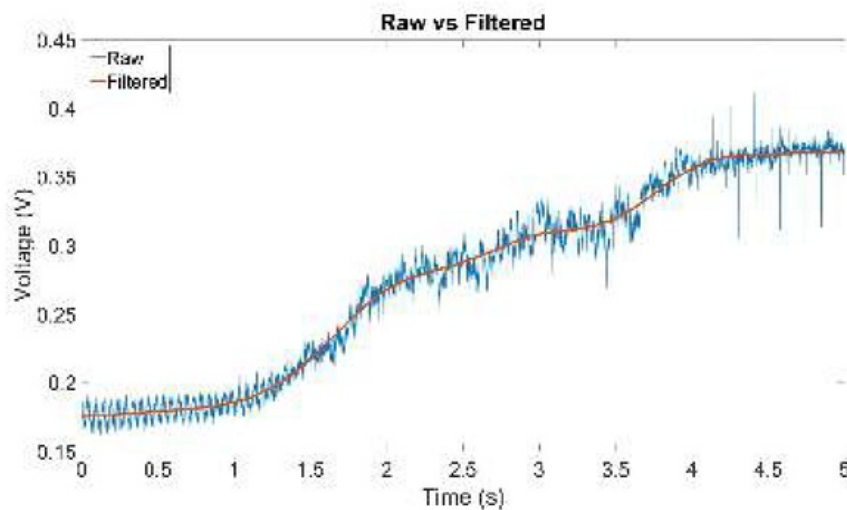


(b) Raw Vs Filtered Data For Comparison of Powders 10mm into Pocket

Figure A.17: Raw and Raw Vs Filtered Data



(a) Raw Data For Consistency Data With SV 010



(b) Raw Vs Filtered Data For Consistency Data With SV 010

Figure A.18: Raw and Raw Vs Filtered Data

Consultation Meetings Attendance Form

Week	Date	Comments (if applicable)	Student's Signature	Supervisor's Signature
2	9/8/16	attend	B. [Signature]	A. [Signature]
2	12/8/16		B. [Signature]	A. [Signature]
3	16/8/16		B. [Signature]	A. [Signature]
4	23/8/16		B. [Signature]	A. [Signature]
5	30/8/16		B. [Signature]	A. [Signature]
6	6/9/16		B. [Signature]	A. [Signature]
7	27/9/16		B. [Signature]	A. [Signature]
8	4/10/16		B. [Signature]	A. [Signature]
9	11/10/16		B. [Signature]	A. [Signature]
10	18/10/16		B. [Signature]	A. [Signature]
11	25/10/16		B. [Signature]	A. [Signature]
12	2/11/16		B. [Signature]	A. [Signature]

Appendix B

Tables

B.1

Equations used for Table B.2 are shown below in Equation C.1, Equation C.2, Equation C.3, Equation C.4.

Property	Value	Source
Kinematic Viscosity at 20 degrees	1.511E-5 ($\frac{m^2}{s}$)	[47]
hydraulic Diameter	0.015 (m)	cite the sketches
Area	2.25E-4 (m^2)	cite sketches
Development Length	0.21 (m)	cite sketches

Table B.1: Properties Used in Theoretical Calculations

Reynolds Number	Velocity (m/s)	ϵ	Length Scale	Time Scale	Velocity Scale
1000	1.007	4.867437	0.000163	0.001761903	0.092606
2000	2.015	38.93949	9.70E-05	0.000622927	0.155745
3000	3.022	131.4208	7.16E-05	0.000339078	0.211097
4000	4.029	311.516	5.77E-05	0.000220238	0.261931
5000	5.037	608.4296	4.88E-05	0.000157589	0.309648
6000	6.044	1051.366	4.26E-05	0.000119882	0.355021
7000	7.051	1669.531	3.79E-05	9.51E-05	0.398533
8000	8.059	2492.128	3.43E-05	7.79E-05	0.440513
9000	9.066	3548.361	3.14E-05	6.53E-05	0.481197
10000	10.073	4867.437	2.90E-05	5.57E-05	0.520764

Table B.2: Kolmogorov's Length, Time and Velocity Scale

Appendix C

Equations

$$\epsilon \approx \frac{u^3}{L} \quad (C.1)$$

ϵ = Average Rate of Dissipation of Turbulence Kinetic Energy per Unit Mass, u = Velocity, L = Development Length

$$\eta = \frac{v^{3\frac{1}{4}}}{\epsilon} \quad (C.2)$$

η = Kolmogorov Length Scale, v = Kinematic Viscosity, ϵ = Average Rate of Dissipation of Turbulence Kinetic Energy per Unit Mass

$$\tau_\eta = \frac{v^{\frac{1}{2}}}{\epsilon} \quad (C.3)$$

τ_η = Kolmogorov Time Scale, v = Kinematic Viscosity, ϵ = Average Rate of Dissipation of Turbulence Kinetic Energy per Unit Mass

$$\mu_\eta = (v * \epsilon)^{\frac{1}{4}} \quad (C.4)$$

μ_η = Kolmogorov Velocity Scale, v = Kinematic Viscosity, ϵ = Average Rate of Dissipation of Turbulence Kinetic Energy per Unit Mass

Bibliography

- [1] 2010. [Online]. Available: <http://www.oindpnews.com/wp-content/uploads/2011/02/Copley-assessing-dry-powder-inhalers.pdf>
- [2] C. Dunber, A. Hickey, and P. Holzner, "Dispersion and characterization of pharmaceutical dry powder aerosols," *KONA Powder and Particle Journal*, vol. 16, no. 0, pp. 7–45, 1998.
- [3] 2016. [Online]. Available: <https://www.innopharmalabs.com/tech/applications-and-processes/particle-size-distribution>
- [4] 2016. [Online]. Available: <http://advancedphotonix.com/wp-content/uploads/SD112-42-11-221.pdf>
- [5] 2016. [Online]. Available: https://www.atp-instrumentation.co.uk/images/manuals/airflow/AVM-8880_manual.pdf
- [6] 2016. [Online]. Available: https://www.newport.com/medias/sys_master/images/images/hb5/hff/8797245177886/R-30990-LHRR-0500.pdf
- [7] 2016. [Online]. Available: <https://www.blackwoods.com.au/part/06366117/regulator-smc-ar20-02-b-14-bsp-17-scfm>
- [8] 2016. [Online]. Available: <http://au.rs-online.com/web/p/flow-sensors-switches-indicators/4487467/>
- [9] A. B. of Statistics, "Australian health survey: First results, 2014-15," 2015.
- [10] 2016. [Online]. Available: <http://lungfoundation.com.au/wp-content/uploads/2015/12/COPD-Backgrounder-2016.pdf>
- [11] N. Islam and M. Cleary, "Developing an efficient and reliable dry powder inhaler for pulmonary drug delivery a review for multidisciplinary researchers," *Medical Engineering & Physics*, vol. 34, no. 4, pp. 409–427, 2012.
- [12] W. H. Finlay, *The mechanics of inhaled pharmaceutical aerosols*. Academic Press, 2001.

- [13] A. I. of Health and Welfare, *Mortality from asthma and COPD in Australia*. Australian Institute of Health and Welfare, 2016.
- [14] P. Correll, L. Poulos, R. Ampon, H. Reddel, and G. Marks, "Respiratory medication use in australia 20032013: treatment of asthma and copd," *Cat. no. ACM 31*, 2015.
- [15] S. Newman, "Principles of Metered-Dose Inhaler Design," *Respiratory Care*, vol. 50, no. 9, pp. 117–1179, 2005.
- [16] M. Hoppentocht, P. Hagedoorn, H. Frijlink, and A. de Boer, "Technological and practical challenges of dry powder inhalers and formulations," *Advanced Drug Delivery Reviews*, vol. 75, pp. 18–31, 2014.
- [17] N. Islam and E. Gladki, "Dry powder inhalers (dpis)a review of device reliability and innovation," *International Journal of Pharmaceutics*, vol. 360, no. 1-2, pp. 1–11, 2008.
- [18] M. Telko and A. Hickey, "Dry powder inhaler formulation," *Respiratory Care*, vol. 50, no. 9, pp. 1209–1227, 2005.
- [19] R. D. Negro, "Dry powder inhalers and the right things to remember: a concept review," *Multidisciplinary Respiratory Medicine*, vol. 10, no. 1, 2015.
- [20] 2016. [Online]. Available: <http://www.asthmaaustralia.org.au/nsw/about-asthma/what-is-asthma>
- [21] 2016. [Online]. Available: <http://asthma.bsd.uchicago.edu/sample-page/asthma/how-asthma-works/>
- [22] 2016. [Online]. Available: <http://www.healthline.com/health/copd/drugs#Overview1>
- [23] X. Kou and X. Cao, "Review of dry powder inhaler devices," *American Pharmaceutical Review*, vol. 19, no. 3, 2016.
- [24] M. Soltani and G. Ahmadi, "On particle adhesion and removal mechanism in turbulent flows," *J. Adhesion Sci. Technol*, vol. 8, pp. 763–785, 2016.
- [25] E. Internet, "Pharmaceutical grade lactose," 2016. [Online]. Available: <http://www.dfepharma.com/en/Excipients/Lactose.aspx>
- [26] M. Coates, H. Chan, D. Fletcher, and H. Chiou, "Influence of mouthpiece geometry on the aerosol delivery performance of a dry powder inhaler," *Pharmaceutical Research*, vol. 24, no. 8, pp. 1450–1456, 2007.
- [27] R. Tuley, J. Shrimpton, M. Jones, R. Price, M. Palmer, and D. Prime, "Experimental observations of dry powder inhaler dose fluidisation," *International Journal of Pharmaceutics*, vol. 358, no. 1-2, pp. 238–247, 2008.

- [28] W. Wong, D. Fletcher, D. Traini, H. Chan, and P. Young, "The use of computational approaches in inhaler development," *Advanced Drug Delivery Reviews*, vol. 64, no. 4, pp. 312–322, 2012.
- [29] M. Coates, H. Chan, D. Fletcher, and J. Raper, "Effect of design on the performance of a dry powder inhaler using computational fluid dynamics. part 1: Grid structure and mouthpiece length," *Journal of Pharmaceutical Sciences*, vol. 93, no. 11, pp. 2863–2876, 2004.
- [30] —, "Effect of design on the performance of a dry powder inhaler using computational fluid dynamics. part 2: Air inlet size," *Journal of Pharmaceutical Sciences*, vol. 95, no. 6, pp. 1382–1392, 2006.
- [31] M. Donovan, S. Kim, V. Raman, and H. Smyth, "Dry powder inhaler device influence on carrier particle performance," *Journal of Pharmaceutical Sciences*, vol. 101, no. 3, pp. 1097–1107, 2012.
- [32] M. Coates, H. Chan, D. Fletcher, and J. Raper, "Influence of air flow on the performance of a dry powder inhaler using computational and experimental analyses," *Pharmaceutical Research*, vol. 22, no. 9, pp. 1445–1453, 2005.
- [33] A. Voss and W. Finlay, "Deagglomeration of dry powder pharmaceutical aerosols," *International Journal of Pharmaceutics*, vol. 248, no. 1-2, pp. 39–50, 2002.
- [34] S. Newman and W. Busse, "Evolution of dry powder inhaler design, formulation, and performance," *Respiratory Medicine*, vol. 96, no. 5, pp. 293–304, 2002.
- [35] T. Srichana and G. M. C. Marriott, "Dry powder inhalers: The influence of device resistance and powder formulation on drug and lactose deposition in vitro," *Journal of Pharmaceutical Sciences*, vol. 7, no. 1, pp. 73–80, 1998.
- [36] M. Telko and A. Hickey, "Aerodynamic and electrostatic properties of model dry powder aerosols: a comprehensive study of formulation factors," *AAPS PharmSciTech*, vol. 15, no. 6, pp. 1378–1397, 2014.
- [37] Y. Kawashima, T. Serigano, T. Hino, H. Yamamoto, and H. Takeuchi, "Effect of surface morphology of carrier lactose on dry powder inhalation property of pranlukast hydrate," *International Journal of Pharmaceutics*, vol. 172, no. 1-2, pp. 179–188, 1998.
- [38] V. Le, T. H. Thi, E. Robins, and M. Flament, "Dry powder inhalers: Study of the parameters influencing adhesion and dispersion of fluticasone propionate," *AAPS PharmSciTech*, vol. 13, no. 2, pp. 477–484, 2012.
- [39] S. Behara, I. Larson, P. Kippax, P. Stewart, and D. Morton, "Insight into pressure drop dependent efficiencies of dry powder inhalers," *European Journal of Pharmaceutical Sciences*, vol. 46, no. 3, pp. 142–148, 2012.

- [40] F. Lavorini, A. Magnan, J. C. Dubus, T. Voshaar, L. Corbetta, M. Broeders, R. Dekhuijzen, J. Sanchis, J. Viejo, P. Barnes, C. Corrigan, M. Levy, and G. Crompton, "Effect of incorrect use of dry powder inhalers on management of patients with asthma and copd," *Respiratory Medicine*, vol. 102, no. 4, pp. 593–604, 2008.
- [41] H. Chrystyn, D. Price, M. Molimard, J. Haughney, S. Bosnic-Anticevic, F. Lavorini, J. Efthimiou, D. Shan, E. Sims, A. Burden, C. Hutton, and N. Roche, "Comparison of serious inhaler technique errors made by device-naïve patients using three different dry powder inhalers: a randomised, crossover, open-label study," *BMC Pulmonary Medicine*, vol. 16, no. 1, 2016.
- [42] D. Farkas, M. Hindle, and P. Longest, "Characterization of a new high-dose dry powder inhaler (dpi) based on a fluidized bed design," *Annals of Biomedical Engineering*, vol. 43, no. 11, pp. 2804–2815, 2015.
- [43] 2016. [Online]. Available: <http://www.ni.com/pdf/manuals/374045a.pdf>
- [44] 2016. [Online]. Available: <http://www.ni.com/datasheet/pdf/en/ds-260>
- [45] 2016. [Online]. Available: <http://www.ni.com/datasheet/pdf/en/ds-86>
- [46] 2016. [Online]. Available: http://www.newark.com/pdfs/datasheets/SSI/67R1070.pdf?_ga=1.80640337.799651444.1478075342
- [47] 2016. [Online]. Available: http://www.engineeringtoolbox.com/air-properties-d_156.html.